# ANALYSIS OF QUATERNARY FAULTS AND ASSOCIATED DEFORMATION OF SEDIMENTARY BASIN FILL: INNER CONTINENTAL BORDERLAND OF SOUTHERN CALIFORNIA

---

A Thesis presented to the Faculty of the Graduate School
at the University of Missouri-Columbia

_____

In Partial Fulfillment
Of the Requirements for the Degree

Master of Science

_____

By
JONATHAN THOMAS BENNETT

Drs. Marie-Helene Cormier and Robert Bauer, Thesis Advisors

JULY 2012

The undersigned, appointed by the dean of the Graduate School, have examined the thesis entitled

ANALYSIS OF QUATERNARY FAULTS AND ASSOCIATED DEFORMATION OF SEDIMENTARY BASIN FILL: INNER CONTINENTAL BORDERLAND OF SOUTHERN CALIFORIA

Presented by Jonathan Thomas Bennett,

A candidate for the degree of
Master of Science

and herby certify that, in their opinion, it is worthy of acceptance.

_____
Professor Milene Cormier

_____
Professor Robert L. Bauer

_____
Professor Christopher C. Sorlien

_____
Professor J. Erik Loehr

Amy-

When I look back on my two years at Mizzou. I often get caught up in wondering how did I survive?  It doesn't take me long to think of the answer:

You.

I love you with all of my heart.

You gave me the strength to finish

Thank you.

-Jonathan

# ACKNOWLEDGEMENTS

I would like to use this space to recognize the phenomenal advising staff afforded to me for this thesis. Working and collaborating with three exceptional minds produced the exciting results contained within this text.

Dr. Milene Cormier had tremendous amounts of patience and enthusiasm during the early days of the research process. Thank you for introducing me to marine geology and the inner continental borderland of southern California. Sharing your knowledge as generously as you have allowed the thesis to take shape and become what it is.

Dr. Robert Bauer served as co-adviser with Dr. Cormier but is also one of the reasons I considered applying to the University of Missouri. Dr. Bauer spent several late nights working with me on making my writing more meaningful. Our brainstorming sessions while looking at the cross sections were made better by your wealth of structural knowledge.

Dr. Chris Sorlien introduced me to a piece of software called IHS Kingdom Suite which I used extensively for the thesis. Feeling the force did not come naturally to me as it took numerous sessions of sitting side by side looking at the abundant seismic data loaded into that glorious piece of software. I must also thank Dr. Sorlien for hiring me for the summer which allowed me to finish my thesis.

Thank you to Dr. Erik Loehr for graciously taking the time out of his schedule to serve as the outside reader and defense committee member.

None of this research would have been possible without the scholarships and assistantships provided by the University of Missouri's Geological Sciences department.

Particularly I would like to thank Dr. Miriam Barquero-Molina for allowing me to teach at Branson Field Laboratory this summer. You allowed me to focus on finishing my thesis and enjoy living in Sinks Canyon again.

Thank you to Information Handling Services for providing the Kingdom Suite licenses at no cost to the Geological Sciences Department. Thank you to USGS, Chevron, and Western Geophysical for making all of the seismic reflection data used in this study publicly available.

TABLE OF CONTENTS

LIST OF ILLUSTRATIONS

**ABSTRACT**

The San Andreas fault system is distributed across strike hundreds of kilometers in southern California. This transform system includes offshore faults along the shelf, slope and adjacent basin, comprising part of the Inner California Continental Borderland. Previously, offshore faults have been interpreted as being discontinuous, or certain faults have been interpreted as thrusts between Long Beach and San Diego. Our work, based on ~3000 kilometers of deep-penetration industry multi-channel seismic reflection data (MCS) as well as high resolution U.S. Geological Survey reflection profiles indicate that many of the offshore faults are more geometrically continuous than previously reported including Newport-Inglewood(NI)-San Mateo-Carlsbad(SMC), and Coronado Bank Detachment(CBD)-Descanso faults. We interpret a ~18 km wide right step over from the NI-SMC positive flower structure in the north to the CBD-Descanso negative flower structure in the south adjacent to San Diego. These digital fault and stratigraphic interpretations were gridded and depth converted for modeling displacement and its direction on the San Mateo-Carlsbad fault.

Stratigraphic interpretations of reflection profiles included the ca. 1.8 Ma top Lower Pico (TLP), which was correlated from wells located offshore Long Beach. Four younger Quaternary unconformities (Q1,Q2,Q3,Q4) are interpreted through much of the study area. We correlate the Q horizons to corehole data in Los Angeles harbor and constrain their ages: Q1 is 160-300; ka Q2 is 300 ka; Q3 300-450 ka; and Q4 ~600 ka. These ages are several times older than the stratigraphic age model published by Covault and Romans (2009) and an order

of magnitude older for the top Lower Pico horizon. Fault slip rates modeled using our new ages would be correspondingly slower than would be the case using the previous ages.

We estimate an average right-lateral slip rate of ~0.44mm/yr since 1.8 Ma on the San Mateo-Carlsbad, which had been published as a thrust. Our modeling also indicates that the SMC fault is kinematically continuous for at least 60km through a major bend that is part of the right step over. This change in SMC strike marks a boundary between transpression in the north and transtension in the south and is regionally significant to understanding earthquake hazard and globally significant to understanding distributed fault systems that reactivate pre-existing structure.

## CHAPTER 1: INTRODUCTION

Prominent continental margin fault systems, such as the San Andreas, North Anatolian, and the northern Venezuelan, are characterized by broad regions dominated by strike-slip faulting and deformation of overlying strata. In addition to their tectonic significance, these zones present potential seismic hazards and hydrocarbon exploration targets. Arguably, the most studied of such plate boundaries is the San Andreas Fault system along the western margin of the United States in California (Figure 1). While the San Andreas Fault is the primary structural expression of the Pacific-North American transform plate motion, the boundary between these plates is broad and complex, containing numerous fault systems and provinces. One such province, the Inner Continental Borderland of southern California (ICB) (Figure 2), is

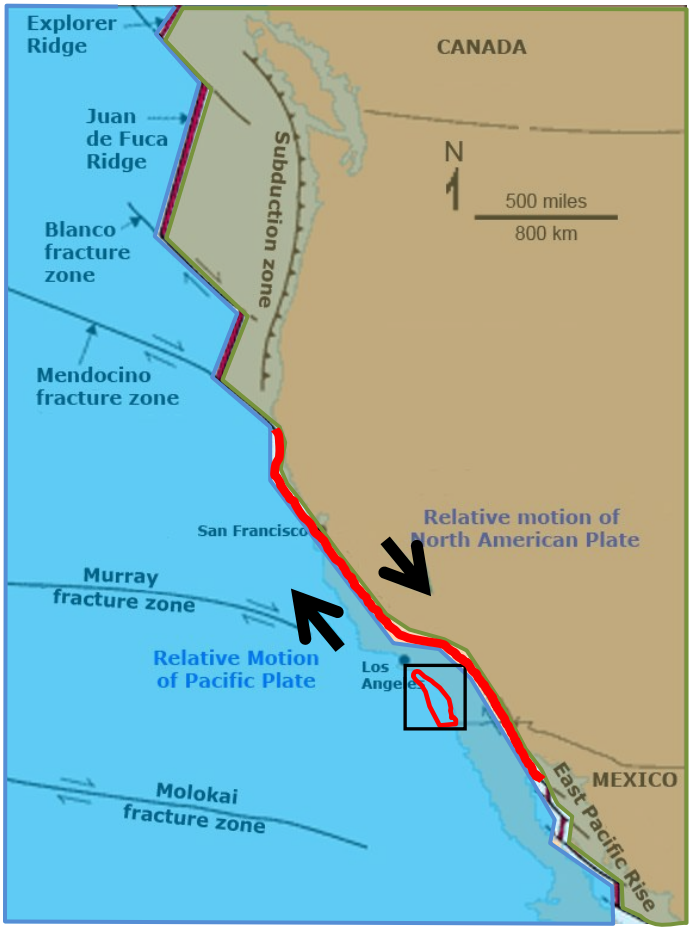


*Figure1*: A regional map showing the location of the San Andreas Fault (Red) overlying the North American Pacific plate boundary. Note the North American Plate is brown and the Pacific plate is blue. The study area is indicated by a red outline with a box framing it. Modified from Stoffer (2006).

characterized by a series of deep, northwest-trending, fault-bounded basins, and uplifted metamorphic basement rocks. Although this broad zone of the Pacific-North American plate boundary accommodates ~52 ± 2 mm/yr of right-lateral shear, most of the slip occurs along the on-shore faults in the region of the San Andreas Fault (Atwater, 1970; DeMets et al., 2000), with some lesser amount of slip accommodated by the offshore fault systems (Beavan et al., 2002). The exact amount of Quaternary slip absorbed by the offshore faults and the relationship of slip to individual faults and their geometries is uncertain since they are under water and are blind in some cases.

The offshore fault zones of the ICB generally includes right-lateral, sub-

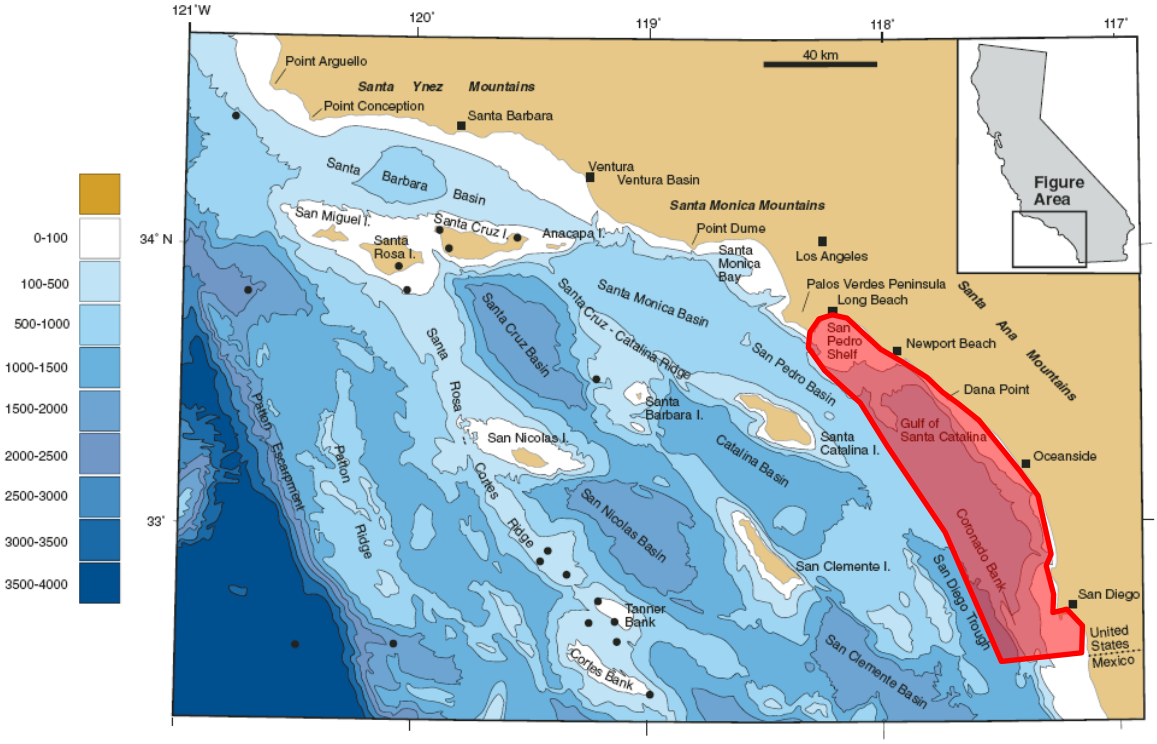


*Figure 2*: A map illustrating the regional geographic features and bathymetry of the Continental Borderland of southern California. The portion of the Inner Borderland of California used for this study area is shaded in red. Modified after Fisher et al., 2009.

parallel strike-slip faults that strike northwest, (Figure 3) (Fisher et al., 2009; Ryan et al. 2009; Rivero and Shaw, 2011; Sorlien et al. 2010). Our understanding of the geometry of these faults has benefited greatly from the recent release of high-resolution industry multi-channel seismic reflection (MCS) data. However, many of the details of the faults and faulting history in the ICB, including their timing, geometry, and activity remain unclear or controversial. To resolve this, more studies using MCS data are needed to interpret: 1.) 3D geometry of fault surfaces, and 2) Quaternary sedimentary horizons.

Stratigraphic continuity of the sediment overlying the faults is complicated by both the complex basin geometries produced by active faulting over time, and by the close proximity of the sediment sources to the confined depositional environments in the ICB (Alexander and Lee 2009; Gorsline, 1992; Normark et al 2009; Warrick and Farnsworth 2009). The primary source of sediment to the ICB is fluvial (Warrick and Farnsworth 2009). A series of rivers along the costal extent of the ICB are responsible for ~80% of the sediment deposited (Warrick and Farnsworth 2009). Most of what is known about the late Quaternary stratigraphy of the ICB is established from piston and box core data acquired on the shelf adjacent to San Pedro and Gulf of Catalina basins (Figure 8) (Normark et al. 2006, 2009) and inferred from ODP drill locations in adjoining basins to the north (Lyle et al., 1997). Pre-Quaternary stratigraphy was established primarily from hydrocarbon wells on San Pedro Shelf, offshore Long Beach (Wright, 1991; Sorlien et al., 2010). Much of the late Quaternary sediments found in the ICB are

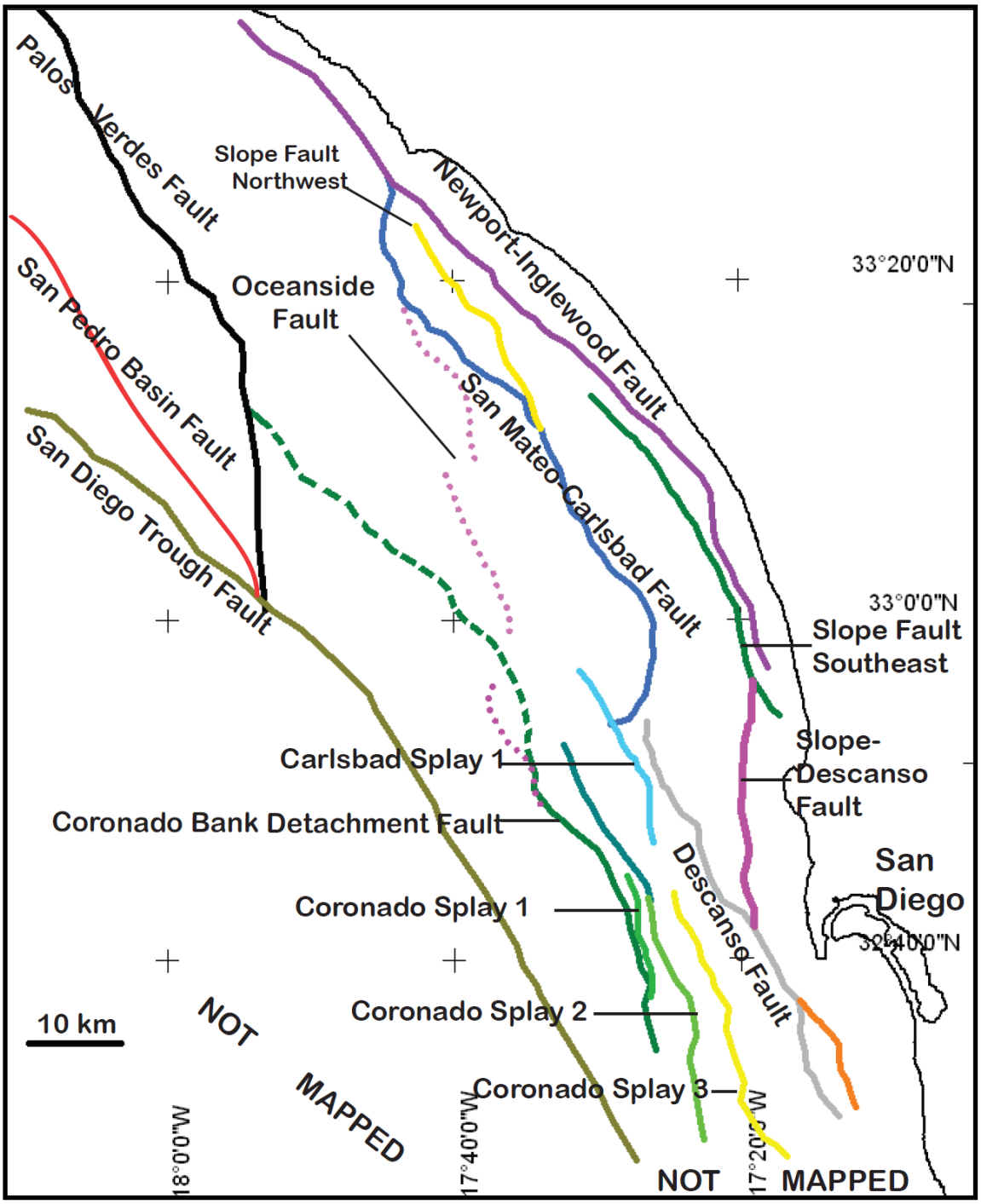


*Figure 3*: A regional map of Quaternary faults indicating the names of the prominent offshore fault systems from this thesis. Certain faults are here newly mapped and others are from Sorlien et al. (2010). The dotted purple lines indicate mapped locations of the Oceanside "thrust" of Rivero et al., 2000 as represented by the Southern California Earthquake Center Community Fault Model (Plesch et al., 2007), as modified by Sorlien et al., 2010.

terrigenous sands and muds. In some cases these materials manifest themselves as submarine fans deposited by turbiditic currents (Normark et al 2009). Research by Covault and Romans (2009) define three prominent turbidite complexes with separate sources in the Gulf of Santa Catalina. Therefore, regional correlations of continuous reflections in seismic profiles based upon lithologies are difficult.(Figures 8 and 24 ).

Even so, efforts to better constrain the age of basin fill sediment across the offshore area extending from Los Angeles to San Diego have occurred (Normark et al., 2009). The quantification of sedimentation rates and patterns from late Pleistocene to Holocene has been tentative—with the age models relying upon extrapolation below stratigraphic control points based on correlation of seismic sequences to eustatic sea level change (Figure 8). However, sedimentation is primarily episodic, dependent on infrequent large storms, landslides, earthquakes, and changes in sea level (Gorsline, 1992). Therefore, integrated on a longer time scale, sedimentation may not be assumed continuous, in part because of tectonic activity.

Understanding fault continuity, activity, and the age and continuity of the basin sediments across the ICB are keys to evaluating both the tectonic history and the potential earthquake hazards associated with these fault systems. The research reported here attempts to contribute to these issues by answering the following questions: *1) Can the Quaternary sedimentary basin fill in the ICB be correlated regionally to dated rocks at petroleum test wells on San Pedro Shelf and scientific core holes in Los Angeles Harbor? 2) What can a reliably*

*dated sediment correlation tell us about fault activity in the ICB? 3) Can a thorough evaluation of the recently released MCS data, paired with a careful interpretation of ICB faults, provide any new insight into the controversies found in the ICB such as slip rates or continuity of faults (Ryan et al., 2009; Jennings et al. 2010; Rivero et al. 2000).*

This study investigates this relationship between Quaternary sediment and the fault systems located in the ICB using the abundant MCS now available, in concert with well data, to constrain ages of the seismic stratigraphy and better define the ICB faults. To resolve this, our study has analyzed over 1500 km of MCS data to assess: 1) fault surfaces, their geometries, and along-strike changes in geometry, and 2) the adjacent Quaternary age sediment horizons—assessing their continuity across the ICB.

The results of this analysis, include: *1) Assessment of the character and continuity of Quaternary age sediments in the ICB using IHS The Kingdom Suite to analyze MCS, well, and bathymetric data; 2) Constraints on the ages of interpreted "horizons" using well data from previous studies; 3) Interpretations of fault surfaces imaged by the MCS data to assess geometry and continuity of ICB faults; 4) Assessment of the nature and timing of the deformation of Quaternary sediments; and 5) Measurement of the structural relief and modeling the sense and direction of displacement along one or more prominent ICB faults.*

Our study indicates that faults in the ICB are more continuous than previously reported (Ryan et al, 2009; Jennings et al., 2010). Some faults such as the San Mateo-Carlsbad, are interpreted here as oblique right-lateral strike-

slip opposed to thrust as previously published. Additionally, this study introduces an alternative age model for near sea floor sediments found in the ICB. Both findings have significant impact on tectonic reconstructions as well as assessment of seismic hazard in the present.

## CHAPTER 2: TECTONIC HISTORY AND REGIONAL GEOLOGY

The present distribution of physiographic, stratigraphic, and structural features observed in the ICB is the result of a series of tectonic episodes that began in the Late Mesozoic. Each tectonic event imprinted the ICB with a set of unique structural characteristics that likely influenced the manner in which subsequent changes in regional stress are accommodated. The tectonic events include: cessation of subduction at ~20 Ma, followed by a period of crustal extension which lasted until ~ 5 Ma, and then by transpression to the Present (Figure 5) (Crouch and Suppe, 1993; Nicholson et al., 1994; Wilson et al., 2009). The sub sections that follow briefly summarize the general tectonic history of the ICB.

### Late Mesozoic-Early Miocene

Subduction of the Farallon plate beneath North America emplaced a zone of lithotectonic belts that comprise some of the oldest rocks in the ICB. These belts include arcs of the Peninsular Ranges and corresponding forearc basin. (Figure 4) (Crouch and Suppe 1993). Numerous subduction-induced thrust faults were created during this time, although it is not known what relationship they share with subsequent episodes of faulting produced during the transition from convergent to transform plate motion. This transition began with transtension, large-scale rifting, and denudation in the early Miocene (Crouch and Suppe 1993). This large-scale rifting and coincident rotation displaced much of the forearc basin which became the Western Transverse Ranges (WTR), and

allowed for rock uplift and denudation of Catalina Schist basement material which is characterized as a metamorphic core complex.

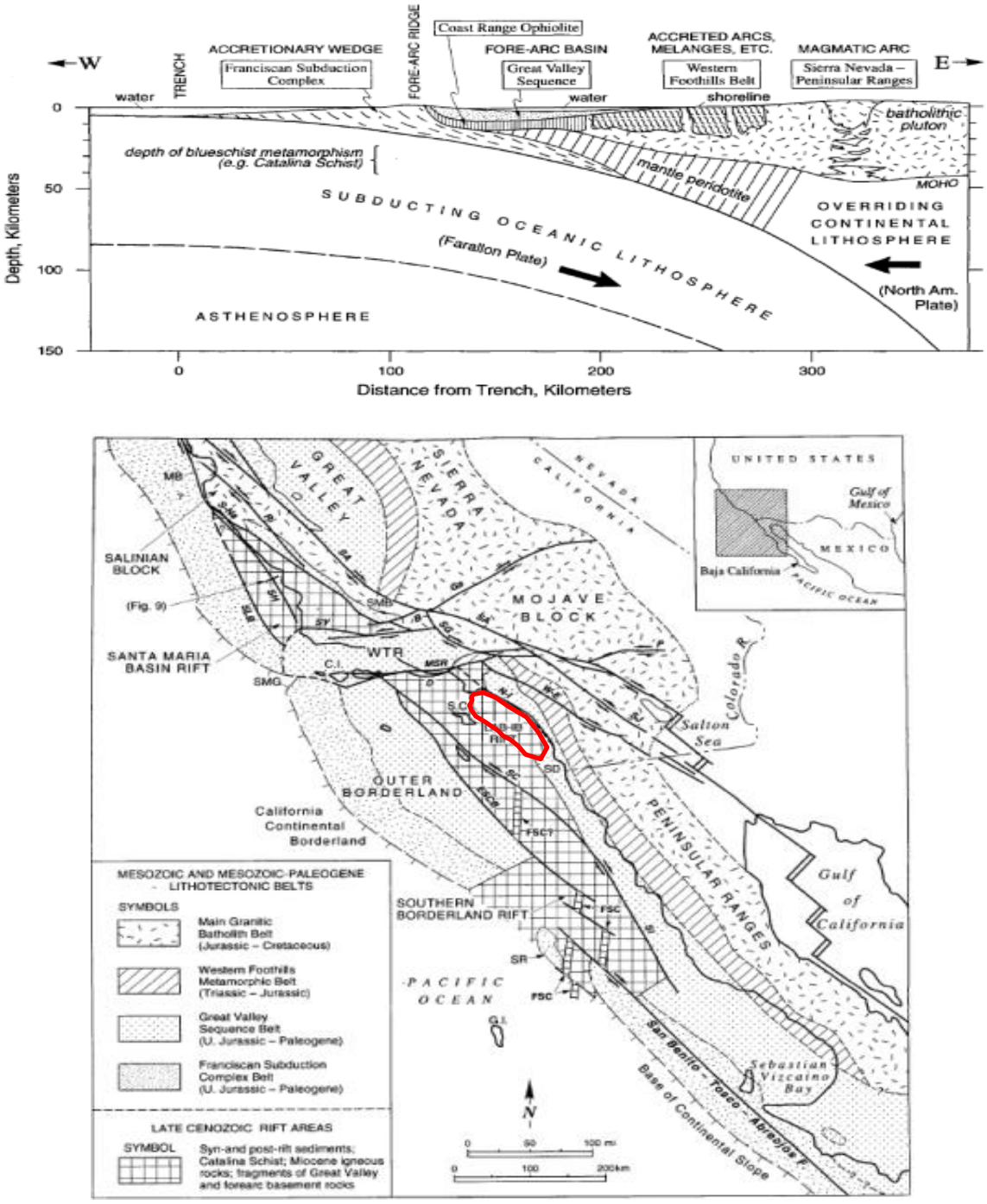


*Figure 4*: (Above) An idealized model illustrating Farallon Plate subduction and the accretion of metamorphic features and their emplacement from Crouch and Suppe, 1993. (Below) A map of the current arrangement of the Mesozoic-Paleogene lithotectonic belts with the study area outlined in red from Crouch and Suppe, 1993.

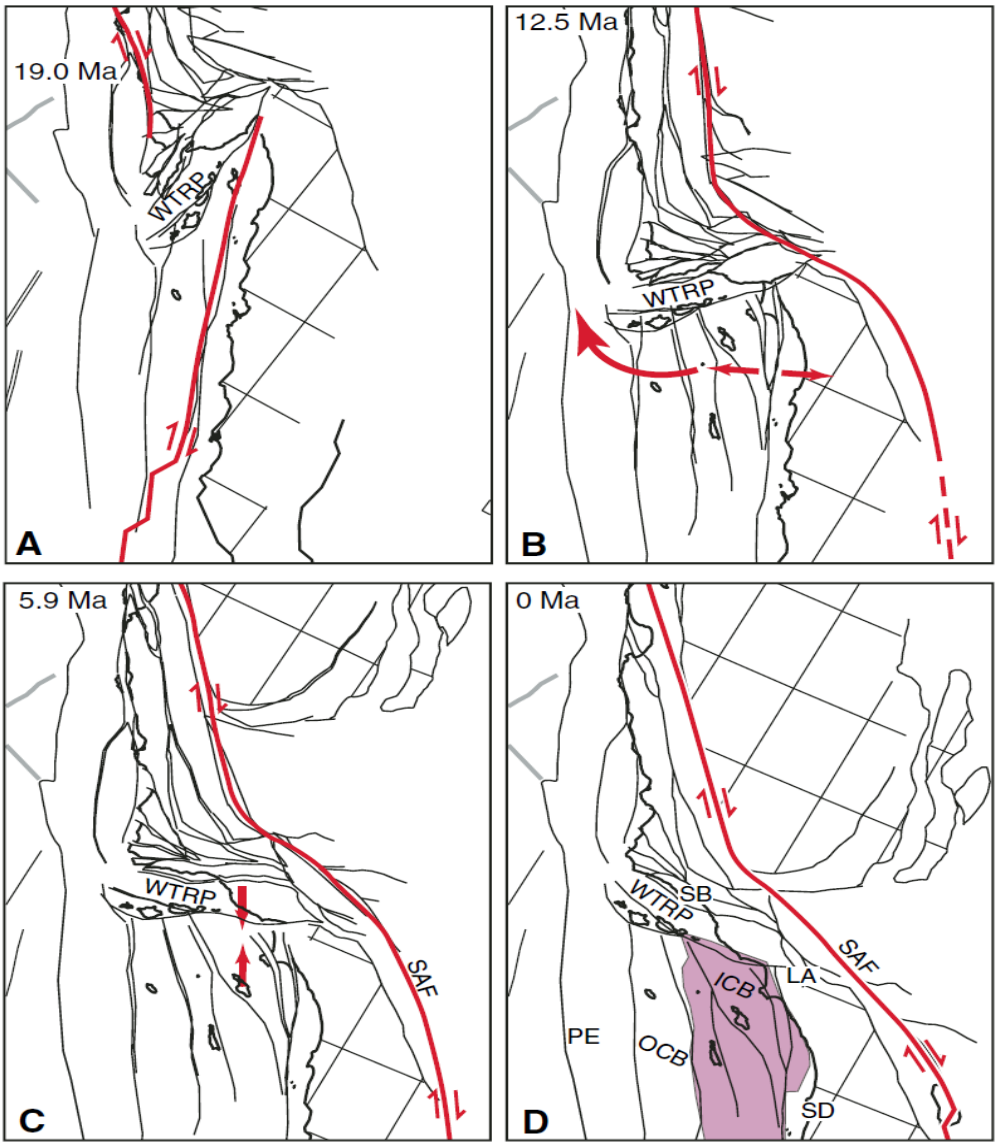


*Figure 5*: A simple tectonic reconstruction of offshore Southern California since the early Miocene (19.0 Ma). (A) Subduction of the microplate remnants of the Farallon Plate ceased in early Miocene. (B) The subduction-emplaced provinces were heated, thinned, and in the case of the Western Transverse Ranges province (WTRP), rotated clockwise 90° (Refer to Figure 6 for more detail) (C) Due to the bend that developed in the San Andreas Fault (Red Line) and therefore the Pacific-North America plate boundary, the northern part of the Inner California Continental Borderland (ICB) underwent transpression or shortening. (D) Catalina Schist that was exposed as one or more metamorphic core complexes shaded in pink. From Fisher et al. (2009).

**Miocene Transtension**

The Miocene epoch is a critical ~15Ma span in the ICB's tectonic evolution which included several important events (Figure 5): 1) initiation of the transition between Farallon-North America subduction and Pacific-North America transform motion (Atwater, 1970; Atwater, 1989; Atwater and Stock 1998). 2) capture by the Pacific Plate of the Monterey microplate and the ensuing rotation of the WTR block (Figure 6) (Kamerling and Luyendyk, 1985; Nicholson et al 1994), and 3) uplift and denudation of basement material (Yeats, 1968; Crouch and Suppe 1993). As the East Pacific Rise (EPR) neared the North America plate, the remaining Farallon plate began to fragment (Atwater 1989; Nicholson et al 1994). The odd elongated shape of the remaining Farallon plate being wedged between the larger Pacific and North America plates caused it to fragment. This also means that the transition from a convergent plate boundary to transform plate motion was not instantaneous and is still an ongoing process in Cascadia and Mexico.

One fragment of the Farallon plate, called the Monterey microplate, partially subducted beneath the WTR block and adhered to that segment of the North America plate. Once Pacific-Monterey spreading ceased, relative plate motion between Monterey and North America changed from oblique subduction to transtensional transform motion. The Monterey microplate then attached to the Pacific plate and began to move with the relative Pacific plate motion. Since the WTR block was still adhered to the Monterey microplate, its separation from the North America plate produced an episode of intense rifting and extension

locally in the ICB (Figures 5B and 6C). Plate motion produced extension that facilitated WTR rotation and local crustal thinning. These processes allowed for the rock uplift and denudation of Catalina schist as well as the formation of basins.

**Late Miocene to Present Transpression**

Transpression, or north-south shortening began ~5 Ma when the main plate boundary shifted to the Gulf of California, the southern San Andreas fault formed, with a major Mojave restraining segment linking to the Central San Andreas Fault, (Crowell, 1979). Large -scale contraction and transpression originated within the western Transverse Ranges and along their southern boundary at the beginning of Pliocene time (Clark et al, 1991; Seeber and Sorlien 2000).

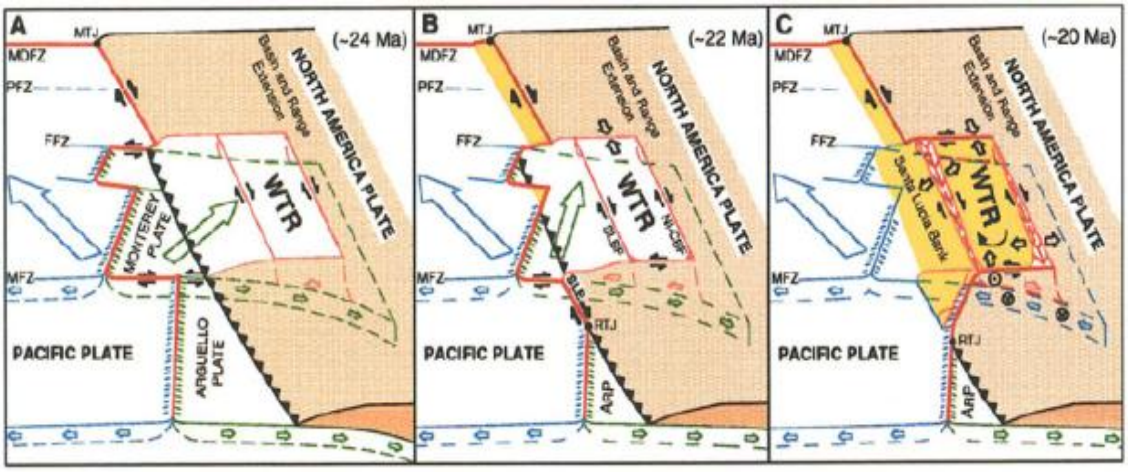


*Figure 6*: A schematic detailing the capture of the Monterey microplate and the subsequent rotation of the Western Transverse Ranges (WTR). The processes illustrated here focus on early Miocene tectonic events from Nicholson et al. (1994). The rift that became the Inner California Continental Borderland is along the right side of the WTR block, labeled NI-CBF on the 22 Ma reconstruction, for Newport-Inglewood-Coronado Bank.

## GEOLOGIC SETTING

### The ICB Fault Systems

The ICB extends from the WTR into Mexican waters in the south. Its western boundary is Santa Cruz - Catalina Ridge and San Clemente Island. The eastern boundary is the southern California coast and Los Angeles Basin (Figure 2). The ICB presently comprises the Catalina province and the western margin of the Los Angeles Basin. Typical continental margins have broad, shallow shelves <120 m deep with gradual slopes as land transitions to the sea. However, the basin-and-ridge physiography that defines the ICB is the result of inverted Miocene extensional basins, uplifted Catalina Schist basement material, and modern basins formed from transpression, and are punctuated by closed-contour basins that reach water depths of >1000 m.

Despite our general understanding of the ICB physiography, our understanding of the geometry of the ICB fault systems and their progressive development has suffered due to inadequate geophysical data available to conduct a detailed analysis and interpretation. As a result, fault representations such as the 2010 Fault Activity Map of California (Figure 7) (Jennings et al., 2010) or the Southern California Earthquake Center Community Fault Map (SCEC CFM) (Plesch et al., 2007) are potentially inaccurate. These maps show ICB fault traces as discontinuous or in some cases do not indicate the presence of other faults altogether. The SCEC-CFM shows continuous faults, but lacks important faults interpreted by Ryan et al. (2009) and Sorlien et al. (2010). These interpretations are critical to our understanding of seismic hazards.

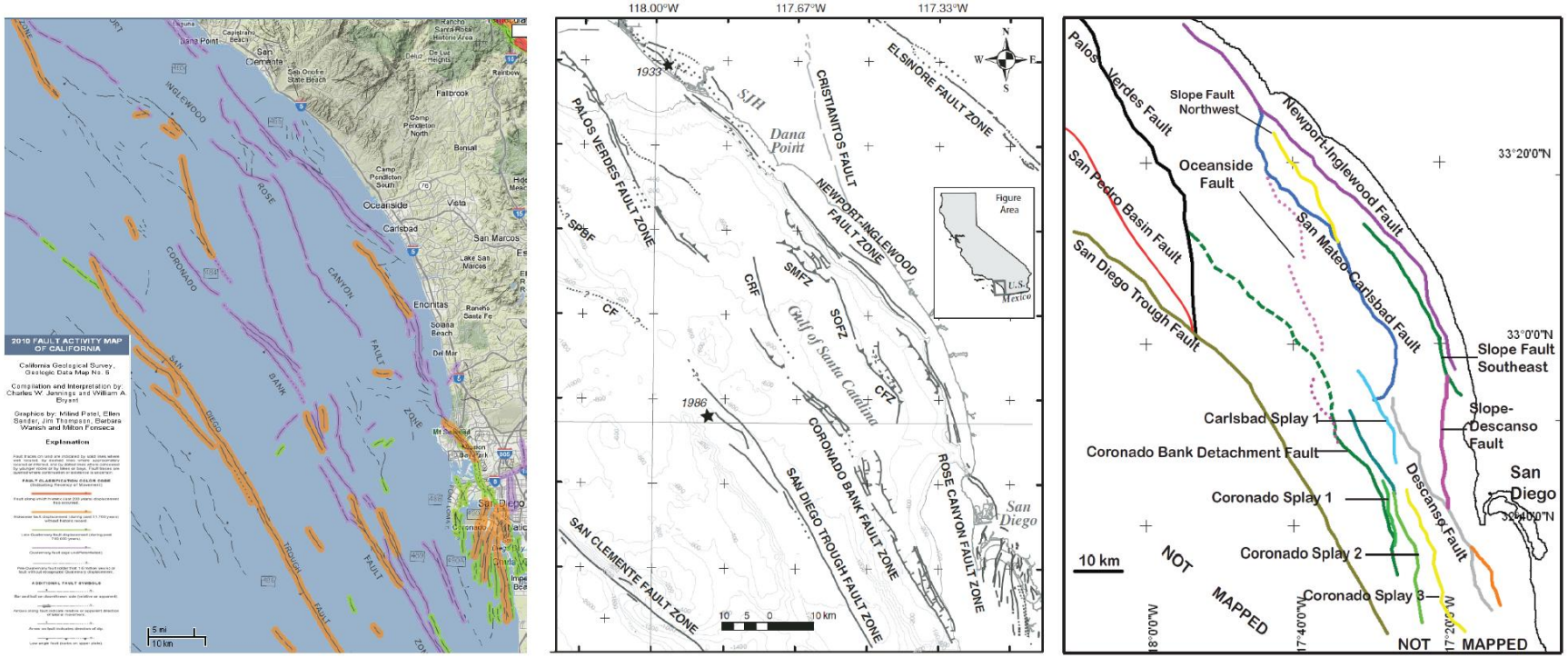


*Figure 7*: A comparison of the 2010 State of California Fault Map (Jennings et al., 2010), the Ryan et al., 2009 map, and the map drawn from this study. There are obvious differences in continuity but also in categorizing the nature of fault activity.

Ryan et al. (2009) published a map showing discontinuous fault traces and did not show certain faults offshore southern California using (Figure 7). Main fault strands were identified using the MCS data sets on the basis of any fault scarps present, changes in dip, and offset or disruption in adjacent reflectors.

The SCEC CFM incorporated the interpretations of Rivero et al. (2000) and Rivero and Shaw (2011), and apparently includes no other interpretations for my thesis area. This is largely because the fault interpretation started in Sorlien et al. (2010) has not yet been provided to SCEC because it was incomplete and not depth converted. Rivero and Shaw (2011) define several faults as blind-thrusts, such as the Oceanside and Thirty-Mile Bank faults. The existence of post-Miocene activity, and/or the slip type, on a large part of the Oceanside thrust and Carlsbad thrust of Rivero et al. (2000) has been questioned (Campbell et al., 2009; Sorlien et al., 2010).

The most direct way to understand the complexity of offshore faults in southern California and the related controversy is to consider these faults as members of either the Newport Inglewood-Carlsbad fault zone in the North or the Coronado Bank-Descanso fault zone in the south adjacent to San Diego. These two fault systems have previously been published as positive and negative flower structures, respectively (Figures 13, 14) (Ryan et al., 2009).

## The Study Area

The extent of this study is bound by the Palos Verdes Peninsula to the North, the California coast to the East, the United States-Mexico border to the South and the Coronado Bank Detachment fault to the West (Figures 3 and 7). This area encompasses much of the same area discussed by Legg (1991); Rivero and Shaw (2000, 2011) and Ryan et al. (2009), which focused on the Newport-Inglewood-Carlsbad and Coronado Bank-Descanso fault zones. These fault zones, while the subject of numerous studies, remain poorly understood and beg to be examined more carefully while considering the complexities of the local Quaternary sedimentation.

## Quaternary Stratigraphy

Gulf of Santa Catalina basin (GSCB) and the San Diego Trough basins are located within this study area (Figure 2). Their close proximity to on-shore sediment sources as well as nearby basins to the north allow for varied sediment source origins. A large amount of the deposition here is due to turbidite or gravity flows from other basins or watershed provinces. Since the GSCB is closed, the turbidite deposition is concentrated, producing spatially distinct deep- sea fans and numerous unconformities (Figures 8, 24). As a result, the submarine fans have separate sources and are localized, making stratigraphic correlations through GSCB difficult.

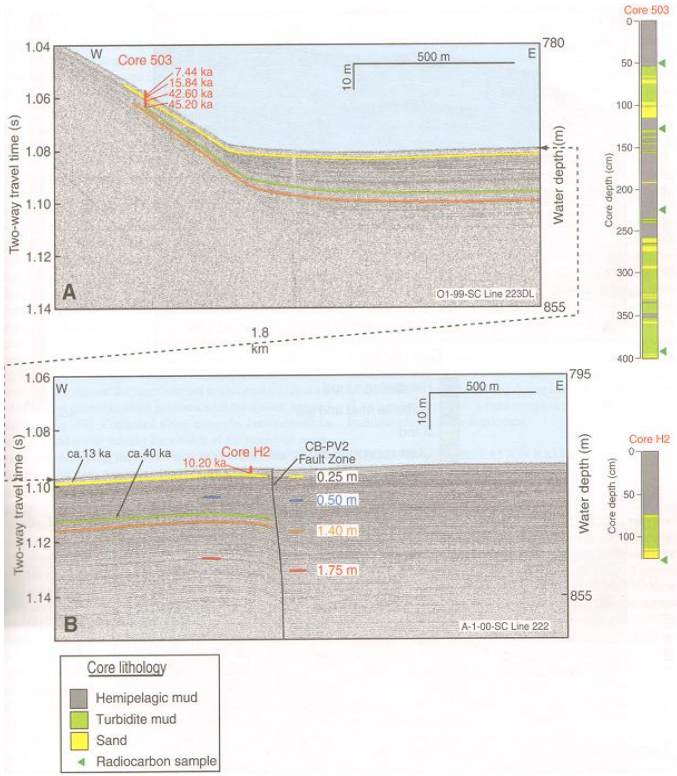


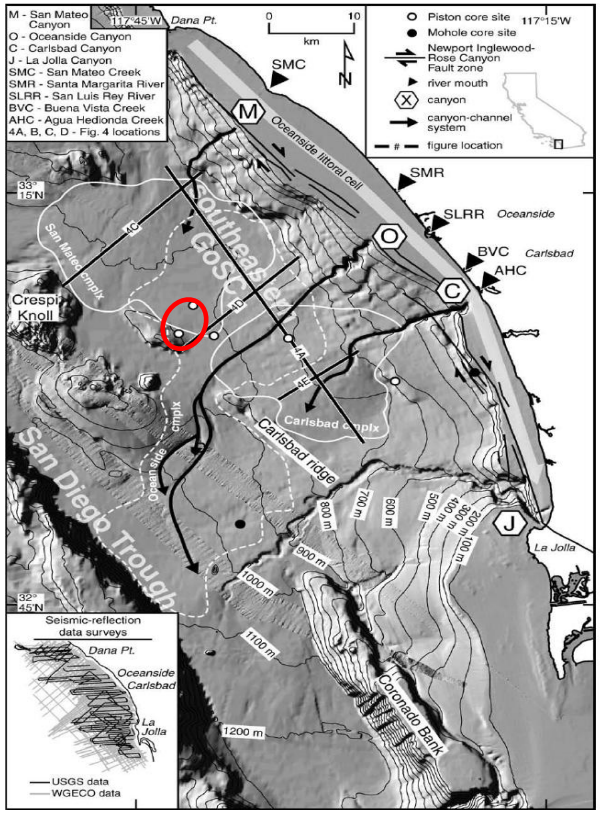


*Figure 8*: Left: Seismic reflection profiles showing the method for dating reflections using radiocarbon-dated cores into the condensed stratigraphic section along the basin edge. Seismic reflection data are then used to correlate reflections into deeper areas in the basin. The cores next to the profiles show alternating thick layers of turbiditic and hemipelagic mud with intermittent thin layers of sand. From Normark et al. (2009). Right: A map showing the locations of deep sea fan complexes drawn on a bathymetric grid. Two of these complexes, the San Mateo and Carlsbad, are mapped as confined within a closed depocenter, whereas the Oceanside complex is mapped as unconfined and bypasses the thesis study area to be deposited in San Diego Trough. The circles located where the San Mateo and Oceanside complexes overlap are the location of the piston cores shown in Figure 8. From Covault and Romans (2009).

A method to date Quaternary sediment was used in studies that tied high-resolution seismic data to radiometric dated sections contained within cores drilled along the edges of basins to provide age constraint in deeper parts of the basin (Figure 8), (Normark et al., 2006a; Normark et al., 2009; Covault and Romans, 2009). Thus, these authors are interpreting, for example, glacial oxygen isotope stage 6 (190 ka-130 ka; Lisiecki and Raymo, 2005) not based on any core data, but instead based on a correlation between the seismic stratigraphy and the global sea level record.

The unconformities within the deep-sea fans of Covault and Romans (2009) may be sequence boundaries and could be used to set age constraints on Quaternary sediments. These unconformities produce unique reflections in MCS profiles that are identifiable in the variable resolution of different data sets (Figure 11) and may be correlated over great distances to core holes in Los Angeles harbor (A to A' in Figure 18) that penetrate most of the Quaternary stratigraphic section (Ponti et al., 2007; Edwards et al., 2009).

## CHAPTER 3: DATA AND METHODS OF ANALAYSIS

### Data Sources

Industry seismic reflection data acquired by Western Geophysical, Chevron, and Jebco, during the late 1970s through the 1980s were made publicly available in recent years through the National Archive of Marine Seismic Surveys (http;//walrus.wr.usgs.gov/NAMSS/index.html). Acquisition of these profiles was designed to image deep (5-6 km) and over a broad area (~30 km offshore) in order to fully characterize the petroliferous Miocene section and the Catalina schist basement. Higher resolution multichannel seismic profiles shot by the USGS in 1998 and 1999 were also made available (Figure 9). Point and multibeam bathymetric data were made available by Dartnell and Gardner (1999), and the National Geophysical Data Center (http://www.ngdc.noaa.gov/mgg/bathymetry/).

Age control needed to assess and constrain fault activity and related deformation was provided from data collected from deep-penetrating hydrocarbon wells south of Los Angeles Harbor, including velocity survey sand Minerals Management Service paleontology available for certain wells ( Sorlien et al., 2010; and unpublished manuscript). This study also used time-depth charts from industry wells along the continental shelf edge.

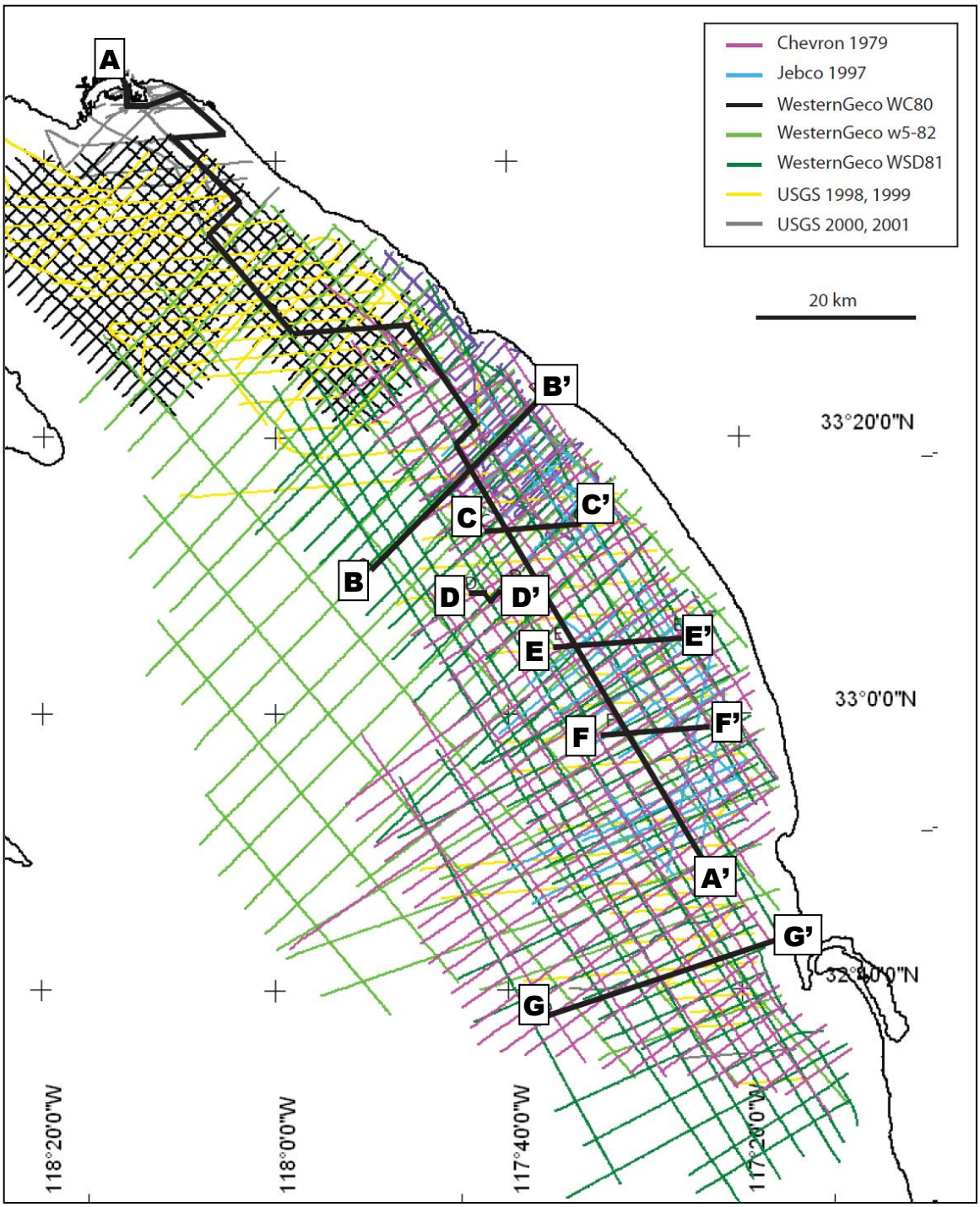


*Figure 9*: The dataset of multichannel seismic reflection (MCS) profiles, identified on the legend. Profiles presented here as figures are located by the labeled heavy black lines.

## Dataset Analysis - The Kingdom Suite

Our interpretation was carried out using an interactive industry software designed for seismic reflection and well interpretation, “The Kingdom Suite”. The aforementioned seismic reflection, bathymetric, and well data were uploaded into a Kingdom Suite interpretation project (Alward et al., 2009; Campbell et al., 2009; this thesis). In order to test the accuracy of the navigation for the seismic reflection data, bathymetric grids were converted to two-way travel time using an interval velocity of 1,490 m/s. The navigation shot-trace number correspondence for the seismic data was then adjusted until a good visual match was obtained between the seafloor reflector and the time-converted bathymetry. Bathymetry was especially critical to successfully loading the Chevron and Western w5-82 data (Campbell et al., 2009, and an unpublished report).

## Stratigraphic Interpretation

Sorlien, et al. (2010) recognized and correlated a ~1.8Ma top Lower Pico (TLP) digital horizon and Pliocene horizon called H4, which they used for preliminary modeling of post-top Lower Pico Quaternary displacements along the San Mateo-Carlsbad Fault (SMC). This distinctive interpreted horizon served as an important boundary for the overlying Quaternary age sediments examined in this study. Reflection pattern recognition and loop-tying techniques were critical to account for vertical and horizontal shifts stemming from 2D migration of dipping strata as well as the disparate resolutions of the various data sets (Figure 11). The 1-2 km spacing of the reflection profiles has allowed for successfully loop-tying fault planes and seismic horizons from profile to profile, yielding some

high confidence in our interpretation of their continuity and geometry. . These interpretation techniques were critical to assessing reflection patterns and their continuity.

Unconformities observed as onlap surfaces on Lasuen Knoll and the footwall of the SMC fault were interpreted systematically throughout the study area. Four unconformities were thus identified and labeled Quaternary1 through Quaternary4 (Q1-Q4) (Figures 10 and 12). The Q4 unconformity is a major onlap surface on the edges of the Gulf of Santa Catalina basin and knolls contained within the study area.

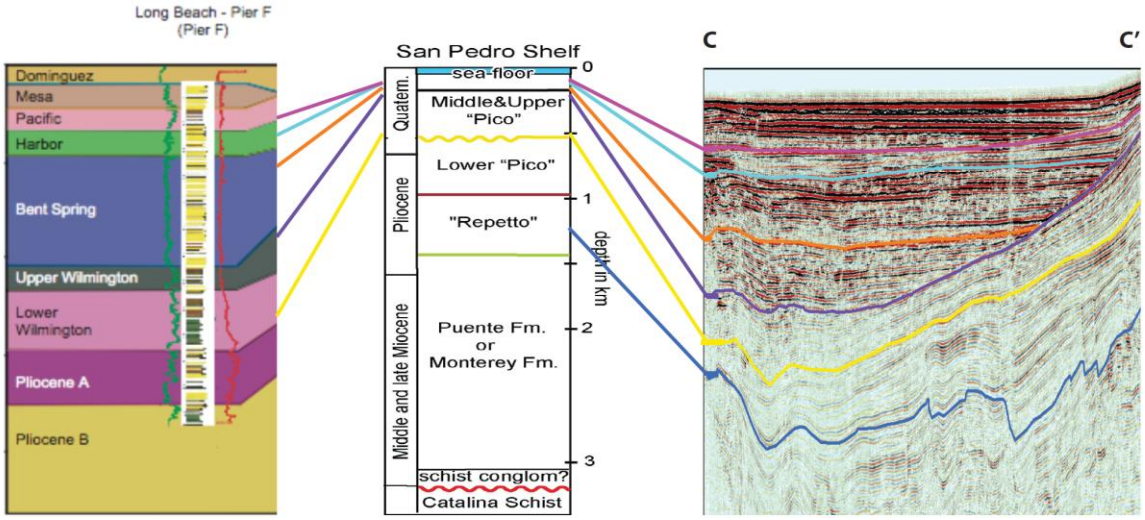


*Figure 10*: USGS high resolution multichannel seismic reflection profile 217 showing the interpreted Quaternary horizons relative to one another located in the footwall southwest of the San Mateo-Carlsbad fault. Quaternary 4 here a major onlap surface representing increasing missing section to the right (east). The stratigraphic column in the center is from Sorlien et al (2010) as modified from Wright (1991) for the downthrown northeast side of the Palos Verdes fault on San Pedro Shelf, south of Long Beach. The Quaternary horizons were correlated as part of this project to a scientific core hole on Pier F of Los Angeles Harbor that was presented by Ponti et al (2007) and Edwards et al., (2009) (Far Left) Refer to Figure 9 for location of C-C'.

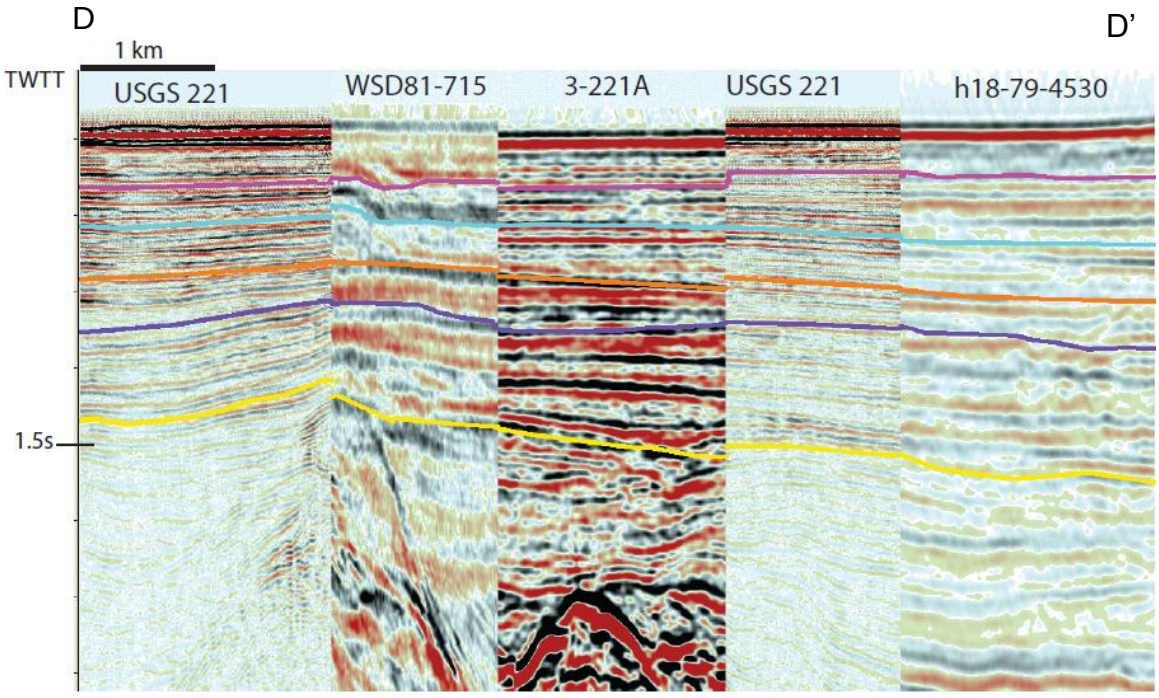


*Figure 11*: A composite profile constructed from high-resolution USGS and deep penetration industry seismic reflection data to illustrate differences in data set resolution. Western Geophysical Company data include WSD81-715 and 3-22A is part of the w5-82 data set on Figure 9; H18-79 is Chevron. This profile also demonstrates how stratigraphic horizons are correlated between profiles and data sets, accounting for small vertical shifts. Refer to Figure 9 for D-D' profile location.

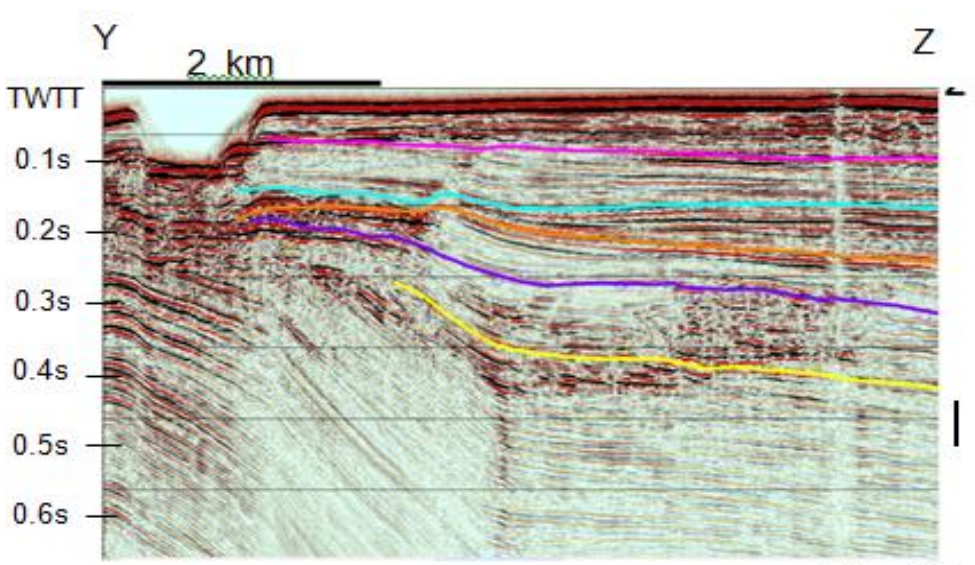


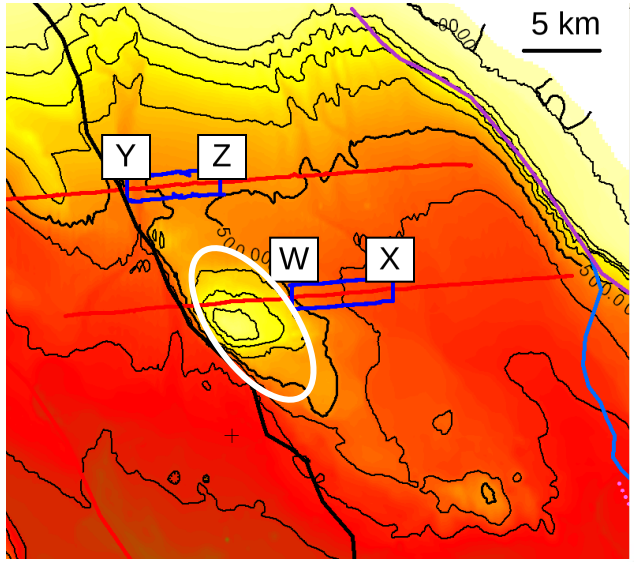


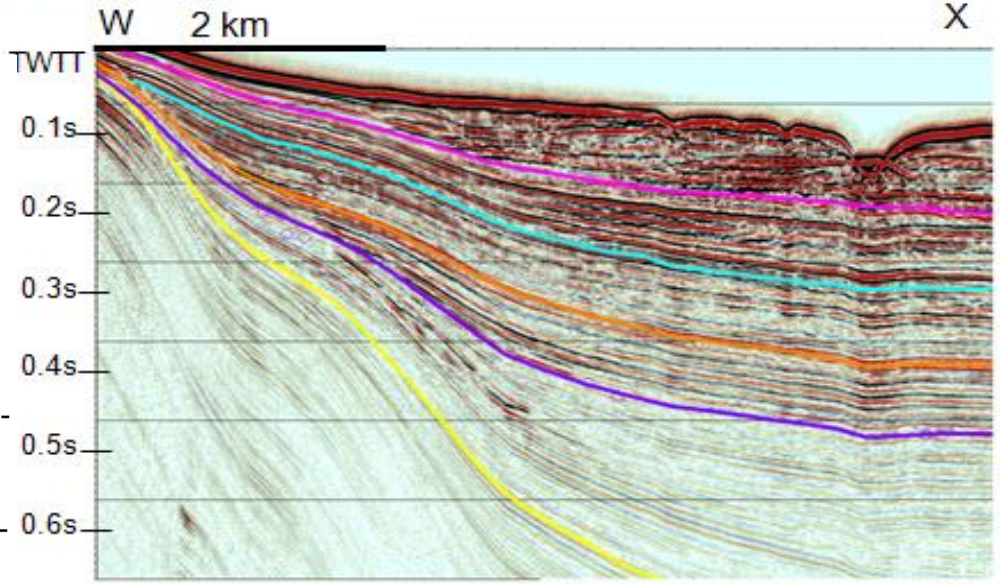


*Figure 12:* Above: USGS high resolution multichannel seismic reflection profile 67 as profile Y-Z shows erosion related to TLP Q4, and Q3. The much steeper dip of TLP vs. Q4 on W-X supports Q4 being much younger, is you assume anything like a constant or only slowly varying tilt rate. Right: USGS high resolution multichannel seismic reflection profile 69 as profile W-X shows the onlap onto Lasuen Knoll of Quaternary 1 – top Lower Pico. The much steeper dip of TLP versus Q4 on w-x supports Q4 being much younger, is you assume anything like a constant or only slowly varying tilt rate. The map inset below shows the locations of Y-Z and W-X and Lasuen Knoll (circle).

**Structural Interpretation**

Published maps illustrating ICB faults show discontinuous faults, incorrect style of activity and/or activity based on Holocene age sediments (Rivero et al., 2000; Ryan et al.,2009; Jennings et al., 2010). Alternative interpretation methods were implemented by workers interpreted ICB faults and a near-base Pliocene horizon (H4) and the ~1.8 Ma Quaternary top Lower Pico (TLP) (Alward et al.,2009; Campbell et al., 2009; Sorlien et al., 2009 and 2010). H4 and TLP provide maximum ages for an alternative age model. Understanding the age of sedimentary horizons associated with interpreted faults provide insight into the timing of fault activity. Therefore, this study focused on improving the existing interpretation of faults located offshore Long Beach and a complete reinterpretation of the faults offshore San Diego by paying closer attention to their

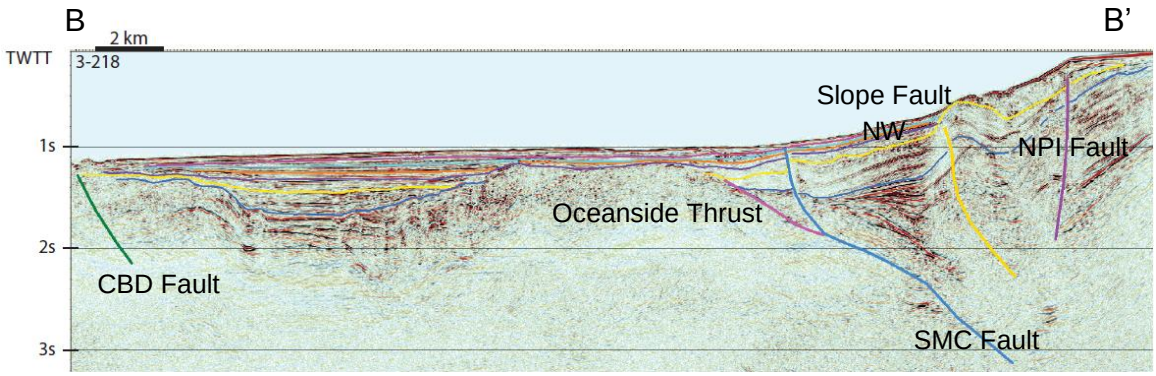


*Figure 13*: Western Geophysical Company 3-218 displayed as profile B-B' in dip orientation showing the geometries of faults and associated folding. The San Mateo-Carlsbad fault forms a positive flower structure with the Newport-Inglewood and intervening faults north of a major right-step over to the negative flower structure presented in Figure 14. From left: Coronado Bank Detachment (CBD); Oceanside (magenta) merging with the San Mateo-Carlsbad (SMC); Slope Fault (Golden Yellow); and the offshore Newport-Inglewood fault (NPI). ~3x vertical exaggeration at seafloor

character and continuity in the MCS data. Specifically, this study focused on the behavior of ICB faults at depth to evaluate their geometries as a fault system rather than as individual faults. Studies such as Oglesby (2005) assessed whether strike-slip step-overs in fault systems impede or enable seismicity. This is significant to the ICB since we interpret a right step-over between the SMC-NPI faults in the north and Coronado-Descanso faults in the south.

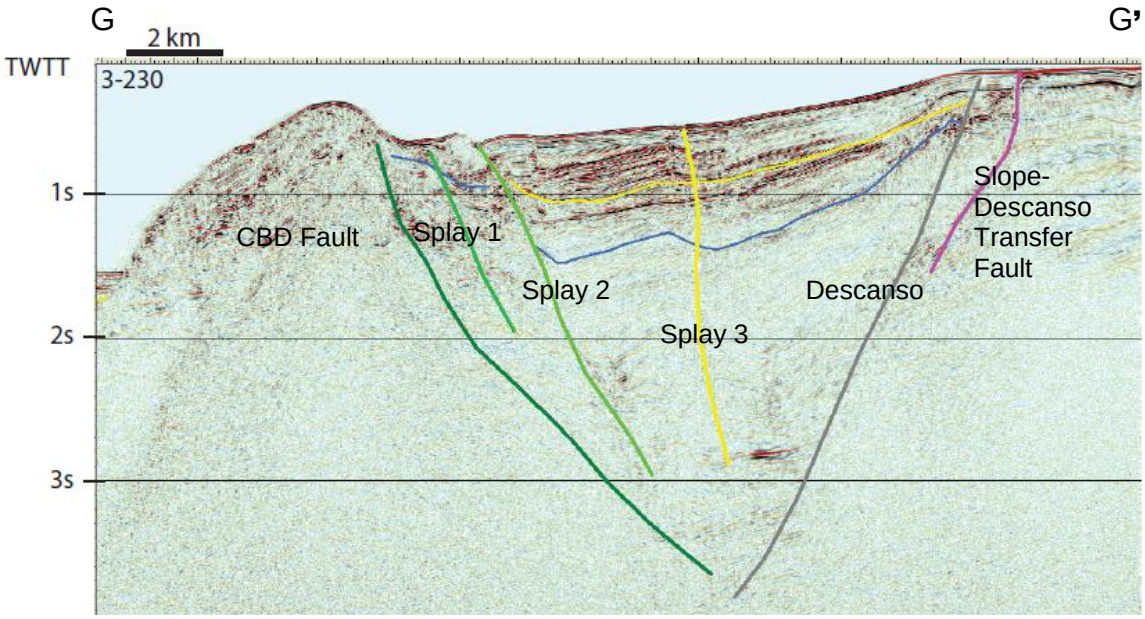


*Figure 14*: Western Geophysical Company 3-230 as profile G to G' showing a negative flower structure geometry adjacent to San Diego consisting of (From Left) Coronado Bank Detachment (dark green); Step over (spring green); Coronado Splay 3(light green); Coronado Splay 4 (yellow); Descanso (gray); and Slope Transfer (Magenta). Profile is shown at ~3x vertical exaggeration measured from sea floor. Refer to Figure 10 for location.

Faults that were deemed most significant were long and continuous (Figure 3) and/or bounded large basins (Figure 14), and/or had large vertical separations of stratigraphic horizons (Figures 13, 14, 15, and 16). Rather than focus on minor splays that die out near the surface, this study focused on faults that deformed strata near the surface but could also be imaged to greater depths. Interpreting fault surfaces and sedimentary reflections required a great deal of patience, precision, and expertise to produce the highest quality results. As such, these were the most time consuming set of tasks in this study.

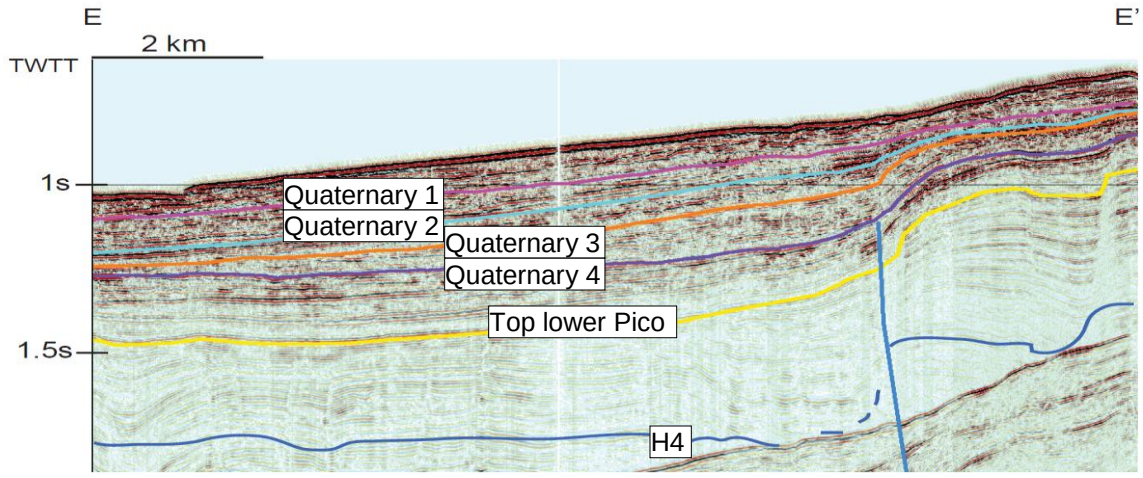


*Figure 15*: USGS high resolution multichannel seismic reflection profile 225 E to E' showing the interpreted Quaternary 1 through Top Lower Pico expressing reverse motion at this location along the San Mateo-Carlsbad fault(blue). Less structural relief is exhibited by the shallower horizons which indicates steady sedimentation during San Mateo Carlsbad fault activity. The Top Lower Pico unconformity caps normal-separation faults in the footwall southwest of the San Mateo-Carlsbad fault, indicating an end to regional transtension in this area at ~1.8 ma (Campbell et al., 2009). The continuous underlying blind faults were interpreted; steeper faults in its hanging-wall cut closer to the sea floor. Normal separation on two of these hanging-wall strands at least up to Q4 is paired with reverse-separation above the main fault, perhaps consistent with right-lateral slip on a more N-S striking releasing segment of the fault. Refer to Figure 9 for location.

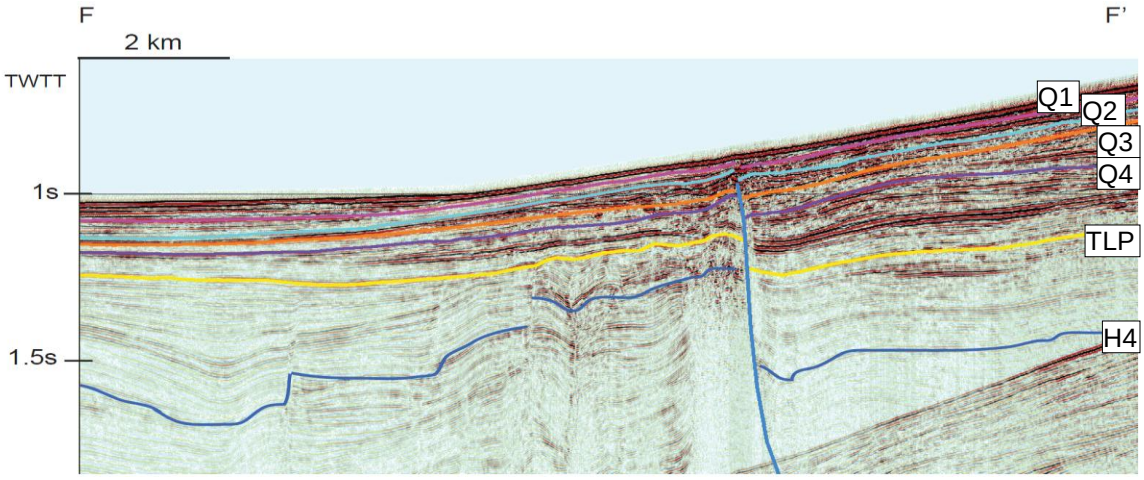


*Figure 16*: USGS high resolution multichannel seismic reflection profile 231 F to F' is located across a the northern bend in the major right step over between the San Mateo Carlsbad fault and the Descanso and Coronado Bank faults. All horizons exhibit normal separation, just 2 km south of profiles illuminating reverse separation. Extension in a right-step over is expected for a right-lateral fault, so the faults segment through this severe bend can be considered a releasing segment. Refer to Figure 9 for location.

## Gridding

Once the interpretations were checked for quality and consistency, 100m two-way travel time grids were created to produce continuous surfaces. The four Q Horizons were gridded in Kingdom Suite using flex grid whereas top Lower Pico and H4 as well as the fault surfaces were gridded using projection of slopes in Surface III (Kansas Geological Survey). These surfaces were viewed in the 3D rendering extension of KS called VuPak (Figure 23).

## Depth Conversion

The time gridded fault surfaces and horizons were depth-converted by producing velocity maps based upon time-depth charts constructed in KS using the software CVM-H provided by the Southern California Earthquake Center (Suess and Shaw, 2003). CVM-H incorporates a SCEC Community Velocity Model (CVM) that has been constructed from high-quality industry seismic reflection profiles and thousands of direct velocity measurements from boreholes from Los

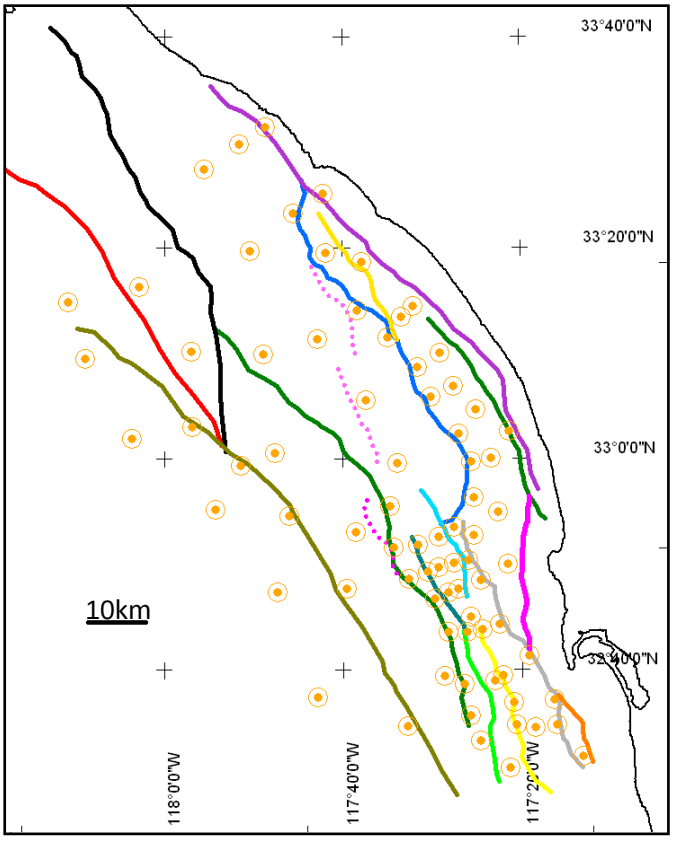


*Figure 17*:Map of the 80 time depth charts constructed in Kingdom Suite software for this project, based on the Harvard 3D velocity model (CVM-H) (Suess and Shaw 2003).

Angeles and velocities derived from stacking velocities during the processing of MCS data (Suess and Shaw, 2003). CVM-H requires coordinates and seafloor depth in order to generate velocity profile for that specific location. Eighty locations were processed in the velocity generating software to create time-depth charts (Figure 17). This provided the basis for depth-converting the interpreted stratigraphic and structural interpretations. (For more information on this model please refer to the Southern California Earthquake Center website: http://structure.harvard.edu/cvm-h)

**Cross-Sections**

Cross-sections were extracted through the gridded fault surfaces and gridded seismic horizons produced with KS at an azimuth of 62˚, which is perpendicular to the approximate strike of interpreted ICB map traces. In all, fifty-eight sections were drawn with each spaced 1km apart. Figure 20 shows the northernmost section (Cross-Section 1) and every fifth section after to illustrate how faults change along strike to the south. Additional cross sections were drawn in 5 km increments to illustrate fault geometries of the faults adjacent to San Diego. Cross-sections were obtained by drawing arbitrary lines across the defined lines and displaying the interpolated trimmed depth-converted fault and sedimentary horizon grids. Refer to the Figure 21's caption for more explanation on this process.

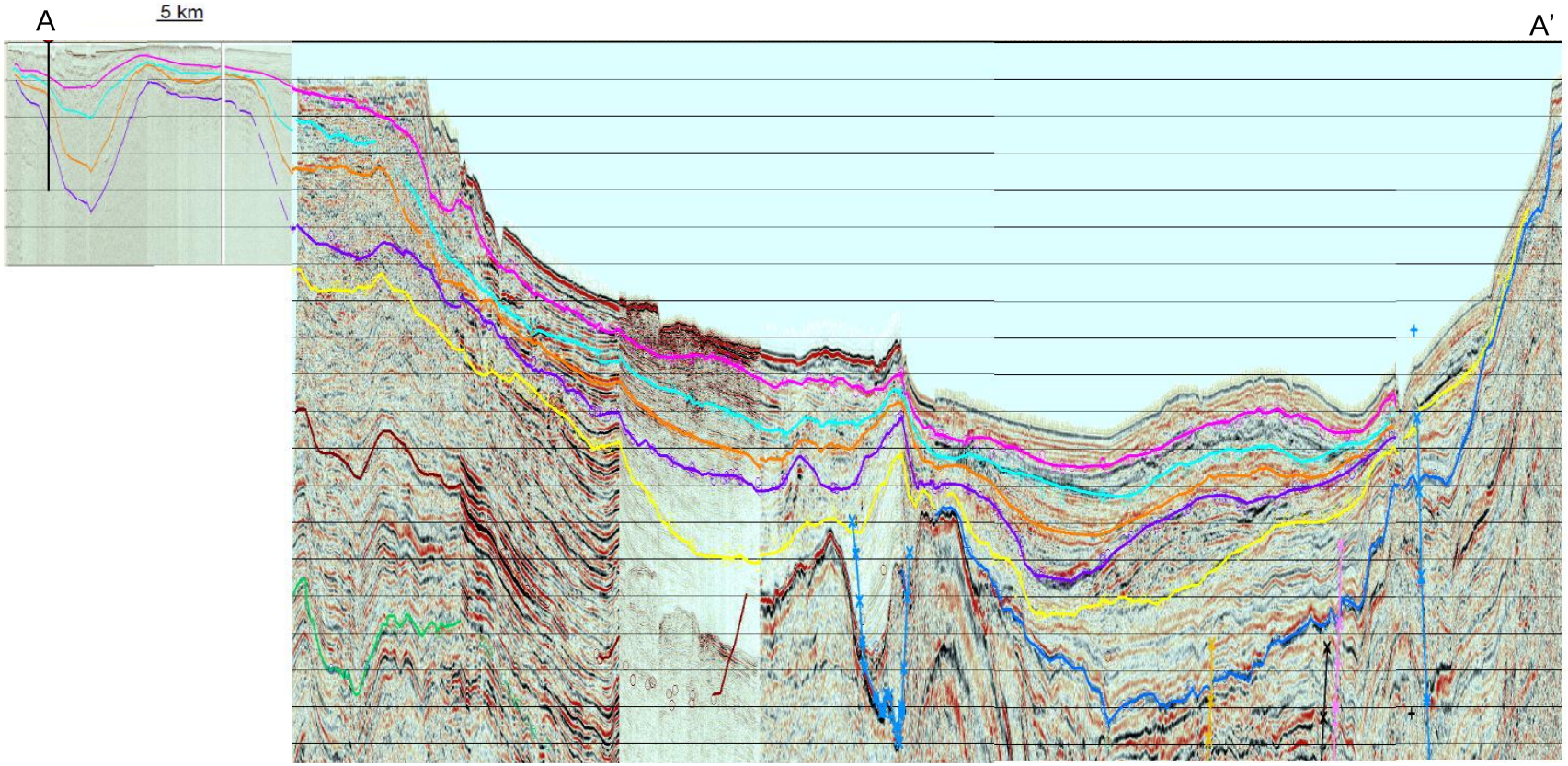


*FIGURE 18*: A composite profile through different multichannel seismic reflection (MCS) datasets, illustrating the 120 km N-S extent of the stratigraphic interpretation of Quaternary 1 through Quaternary 4. A scientific corehole from Pier F in Los Angeles harbor is shown at the north end of the profile. Age and velocity information from Ponti et al (2007) and Edwards et al., (2009) were used to calibrate the stratigraphy of this thesis. Nearby oil exploration wells with Minerals Management Service paleontology and check shots surveys, and a cross section in Wright (1991), were correlated to this profile to constrain the Top Lower Pico and top and base Repetto horizons (Sorlien et al., 2010). The small color circles along each horizon interests represent the numerous intersections ("Ties") to crossing MCS profiles. A single profile through dense grids of MCS data can never adequately represent the actual error-checking of careful work through a volume of data. Refer to Figure 9 for profile location.

## Measurements

For the shallow Q3 and Q4 horizons, vertical deformation across the fault is less than 350 meters and does not extend that far from the San Mateo-Carlsbad fault. Because of this small relief and the possibility of deposition at significantly different depths across the fault trace (expected for the Q1-Q4 strata), and because it was only possible to completely interpret horizons over about 25 km of the hanging-wall of San Mateo-Carlsbad, trigonometric modeling to infer cumulative slip is not expected to be very reliable for these two horizons. Thus, the main goal in mapping the Q horizons is to test whether the overall deformation pattern is similar to that of the deeper TLP horizon - or not. If the deformation pattern is similar, it would support a model where the tectonic regime has not changed significantly since deposition of TLP, and that long term slip directions and rates might therefore extend into the present. In other words, this fault would be an active fault, and the mean slip rate inferred from modeling the deformation of TLP are likely applicable to the Present.

## Procedure for measuring Q3 and Q4

The San Mateo-Carlsbad fault consistently dips to the east; therefore, the footwall is always to the west and hanging wall to the east. The measurements using Q3 and Q4 involved:

1) Carry out a visual inspection of the depth-converted profile to determine if vertical separation is normal or reverse.

2) If reverse separation is observed, as it is in Figure 15, the highest point of the hanging wall within 2 km from upper fault tip is measured and the depth of the

lowest point on the footwall within 1 km of the fault tip is recorded. The vertical relief is the difference between the two depths (Figure 19).

If normal separation is observed (Figure 16), the measurements are reversed: measure depth of lowest point of the hanging wall within 2km of the fault tip.

**Procedure for TLP:**

The procedure for measuring deformation of top Lower Pico follows the same steps as Q3 and Q4. This is not true for the slip modeling as distances from the fault increase to 4km for the hanging wall and 2km for the footwall. These distances were chosen because they visually best captured structural relief of TLP associated with the SMC fault. Care was taken to not make measurements where horizons are not interpreted (i.e., make sure that gridding has not simply interpolated the horizon where it has not been interpreted).

**Apparent Dip of Fault**

Apparent dip for the San Mateo-Carlsbad fault was calculated by measuring the depth of the tip of the fault and the depth of the fault 4,000 meters east of the tip on each of the 58 cross sections in Figure 21. Using equation Apparent Dip =*ATAN[(Depth 4,000m East - Fault Tip Depth)/4,000) ].* In cases where the fault is too steep to measure its depth 4,000 meters East, the depths were instead divided by whatever the maximum measured distance was (Figure 19).

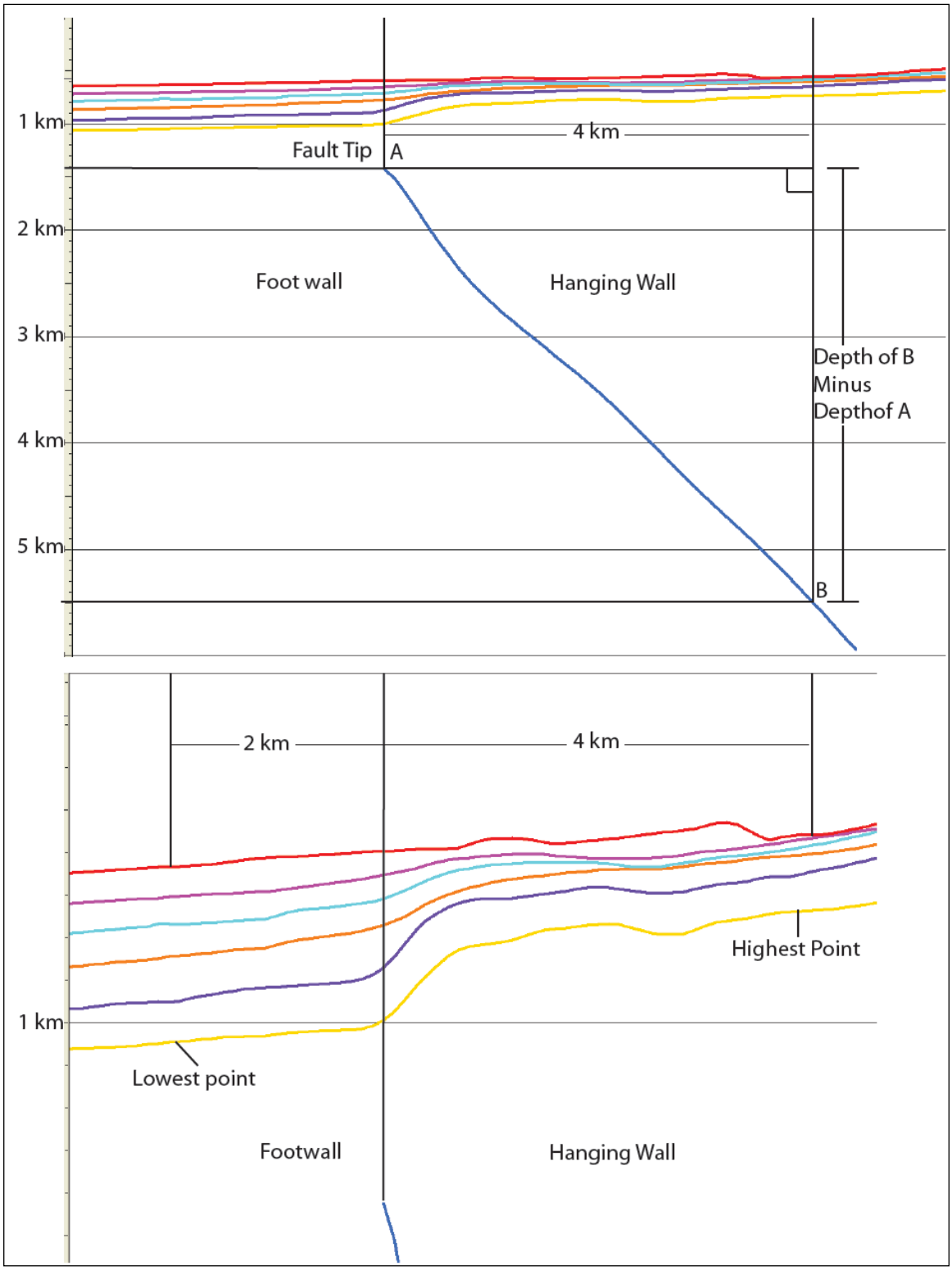


*Figure 19*: Representative cross section from Figure 20 showing how faults dip and structural relief of top Lower Pico were measured for displacement modeling. Top with No vertical exaggeration; bottom shown vertically exaggerated.

**Fault Strike**

Strike of the San Mateo-Carlsbad fault was measured on the 2500 m depth contour at each designated cross section. Strike was then interpolated linearly at 200m increments.

**Slip Modeling**

A simple trigonometric model is used to estimate slip direction and slip magnitude on the San Mateo-Carlsbad fault. This model assumes that vertical motion is due to oblique transport up or down a ramp of apparent dip (Sorlien et al., 2010). Measurements of fault strike and apparent fault dip are compiled into an Excel spreadsheet to calculate the true fault dip of the SMC fault for each cross-section. In turns, these values are used to trigonometrically calculate the expected magnitude of vertical deformation for varying values of the horizontal slip direction of the hanging wall with respect to the footwall:

$$SR=\Sigma_i 1km*\sin(\alpha_i)*\tan(\delta_i)$$

Where $\alpha_i$ is the angle between the local slip vector and local fault strike, and $\delta_i$ is the fault's true dip for cross-section (Figure 20). The slip direction of the hanging-wall, fault strike, and fault dip are used for each 1 km bin along the fault to calculate increase in structural relief for rock passing through each bin (Sorlien et al., 2006).

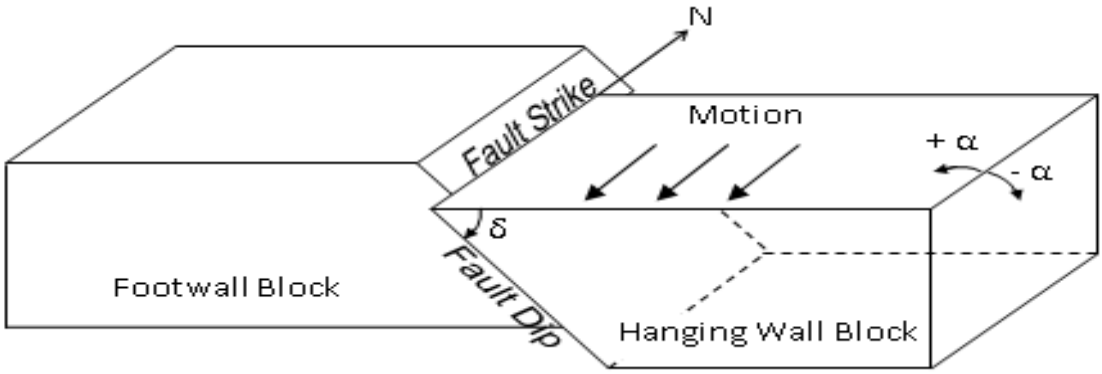


*Figure 20*: A graphical representation for the values in the slip modeling equation $SR=\Sigma_i 1km*\sin(\alpha_i)*\tan(\delta_i)$. This idealized graphic assumes that relative plate motion accommodated by the fault is expressed by movement of the hanging wall block in a predominantly southward motion

**Sources of Error**

Error in the two-way-travel-time structural and stratigraphic interpretations was minimized during this study by being consistent, systematic, and thorough during each step used in the methods. The CVM-H velocity model is based upon stacking velocities for the study area (Suess & Shaw, 2003) and so may contain significant error. The trigonometry used in the slip modeling assumes that the hanging wall is moving rigidly up the apparent dip of the footwall. If the actual structural model for the SMC fault is different, there is some amount of error. Unconformities can be time transgressive and therefore may be of slightly different age in the basin than when dated at wells or cores. Even so, each method of analysis is easily reproducible; therefore, we remain confident that the results produced by this study are based on thorough analyses that have taken into account the aspects of the methods susceptible to error.

## CHAPTER 4: RESULTS

The detailed analysis and measurement of interpreted surfaces based upon the extensive seismic data sets loaded into IHS Kingdom Suite provide new insights into the Quaternary stratigraphy of the ICB, the precise geometry of its fault system, as well as the average slip direction and cumulative displacement across one of its prominent faults. The following sections provide a description of these results.

*1) Assessment of the character and continuity of Quaternary Age sediments by interpreting data loaded into IHS Kingdom Suite.*

Our analysis indicates that the sedimentary horizons referred to here as Quaternary 1 through Quaternary 4 (Q1-Q4) are interpreted as continuous over the area shown in Figures 18 and 30. The deeper Q3 and Q4 horizons appear to be more continuous than Q1 and Q2 over a greater area since they were not disrupted by the numerous channels and canyons that presently carve the seafloor. Our confidence in their continuity is based on the close (1-2 km) spacing of the track lines to one another (Figure 9). This data density allowed for the use of adjacent data sets to avoid onlap, resolution wash-out, and other impediments across the study area.

Quaternary 4 is consistently defined as an onlap surface in the footwall near the San Mateo-Carlsbad (SMC) fault. Q4 and Q3 are sequence boundaries that onlap near the ENE Lasuen Knoll (Figure 12) and on to which younger strata onlap. Q1 and Q2 are sequence boundaries and locally are erosional unconformities as well. Vertical thickness variations between adjacent horizons

occur along the northwest-southeast extent of the study area, as shown by isochore maps produced from the depth converted horizons Figure 30.

*2) Constraints on the ages of interpreted "horizons" using well data from previous studies*

The interpreted Top Lower Pico horizon is estimated to be ~1,800 ka (Sorlien et al., 2010) and thus establish that the ages of subsequent Q horizons were younger than ~1,800 ka . The Q horizons are interpreted as continuous (Figure 18) as far north as wells located in Los Angeles Harbor near Long Beach (Figure 9). The age constraints provided by core holes used by Edwards et al. (2007) indicate that the Q4 is ~580 ka Q3 is ~300-450 ka, Q2 is ~300 ka and Q1 is ~160-300 ka. This differs greatly with reflections at similar depths further south dated by Covault and Romans (2009) that were based upon dates extrapolated by Normark et al (2009). Covault and Romans (2009) show a surface dated 165ka near the same depth of our top Lower Pico at ~1,800 ka (Figure 23). The age difference between these surfaces is over ~1,600 ka, greater than one order of magnitude. Additionally, their shallower surfaces are dated to be much younger than the Q horizons in this study. These disparities are significant since they are used to determine the timing of fault activity.

*3) Interpretations of fault surfaces imaged by the MCS data to assess geometry and continuity of ICB faults*

Careful analysis of the MCS data loaded into Kingdom Suite revealed that most ICB faults are continuous surfaces rather than segmented as previously published (Figure 7). Depth-converted grids produced from fault interpretations produce smooth surfaces—which when examined as 3 dimensional objects—

that are consistent with fault geometries associated with transform margins (Figure 23).

Cross-sections of depth-converted surfaces shown in Figure 21 progress from north to south for 58 km. In the north, these cross sections illustrate how the San Mateo-Carlsbad (SMC), Newport-Inglewood (NI), and the intervening faults converge at depth. The reverse separation and folding indicate that these faults form a positive flower structure. The SMC and NI faults are not imaged consistently deep enough to determine whether they merge at depth or if one cuts the other.

The SMC fault strikes sub-parallel to the other northern faults until cross section 51 (Figure 20). The inset map in Figure 20 shows the SMC strike trends more north-south, which produces a right step-over or bend. Although it remains unclear if this change in orientation is a step-over or a bend, since we do not interpret the SMC fault merging with any faults interpreted further south, it is interpreted here as a 10 km-wide step-over to the Descanso fault. Cross sections 52 through 58 show normal separation of the footwall and hanging wall. This means that the SMC fault strike at this orientation has an extensional component of motion.

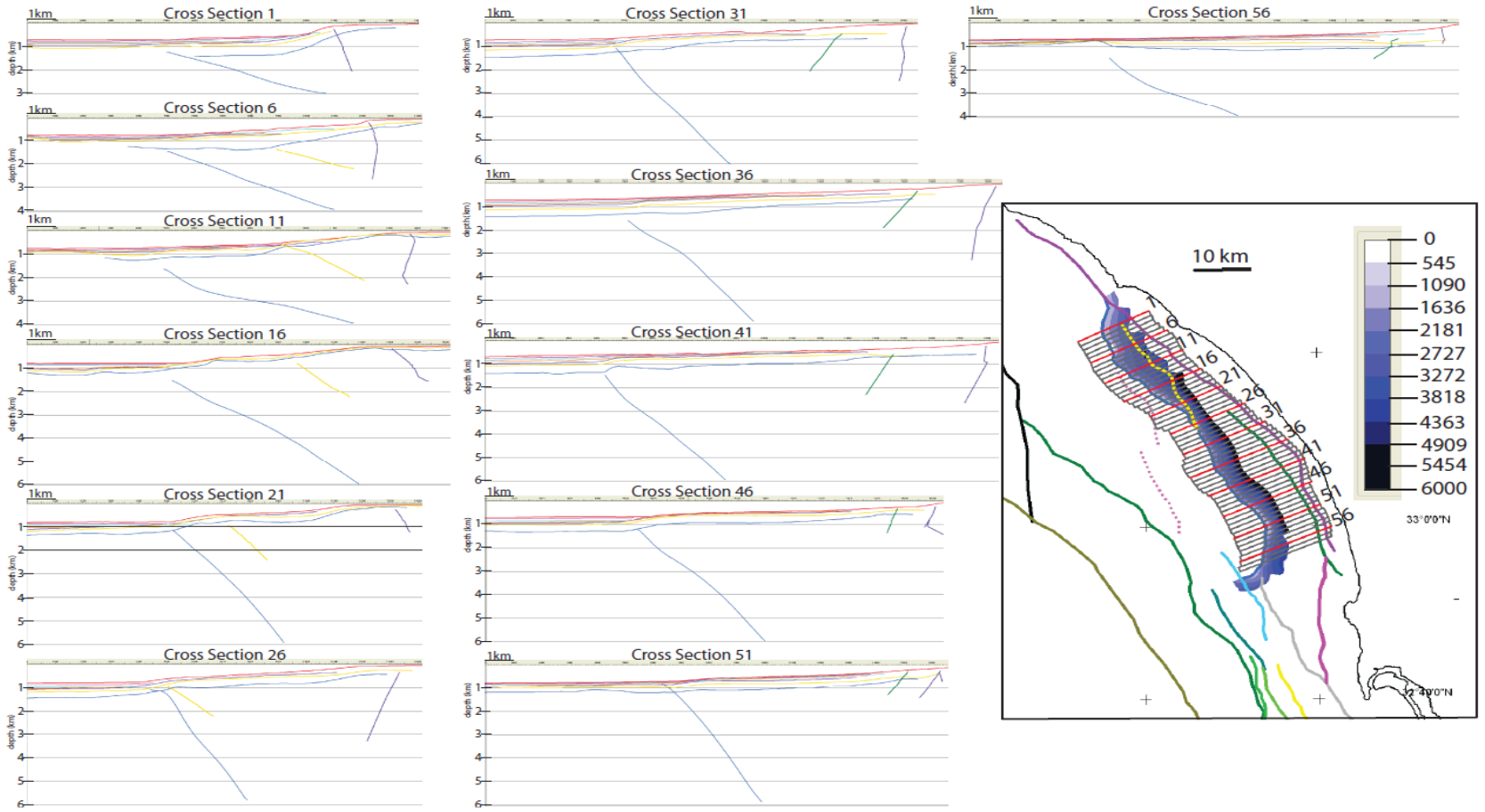


*Figure 21*:Every fifth cross section used for the strike and dip measurements and slip modeling displayed with no vertical exaggeration showing the depth-converted San Mateo-Carlsbad fault(blue); Slope fault NW(yellow); Slope fault SE(dark green); and the Newport-Inglewood fault(violet). Cross sections are displayed in order from north to south. The map shows the depth converted San Mateo Carlsbad as well as the locations for the 58 cross sections spaced 1 km apart, with every fifth one displayed here indicated by a red line.

Figure 22 shows cross sections 1 through 10 (drawn every 5 kilometers) that image the fault systems adjacent to San Diego. Here we interpret a major basin-bounding fault (the Descanso fault) that is absent from both the Jennings et al. (2010) map and the map produced by Ryan et al (2009). The Descanso fault is just south of the bend in the SMC fault and continues past the southern edge of the study area into Mexican waters, where it had been previously interpreted by Legg (1991) (Figures 3, 22, 23). We also interpret a transfer fault that connects the Newport-Inglewood fault southward to the Descanso fault. The Coronado Bank fault zone contains several prominent strands (Figures 3, 21, and 22) ,(Legg, 1991). The Coronado strands are mapped with a left-stepping en-echelon pattern. These faults converge at depth and adjacent sedimentary reflections exhibit normal separation, which indicates that the southern faults form a negative flower structure (Figures 14 and 22).

Figure 21 shows that the SMC fault tends to have a gentler (18-25°) dip to the north while steepening to the south (~55°). The dip of the Coronado Bank fault changes several times from north to south. Many of the secondary faults show changes in dip along strike, while other faults, such as the NI and Descanso, are more consistent in their geometry (Figures 21 and 22).

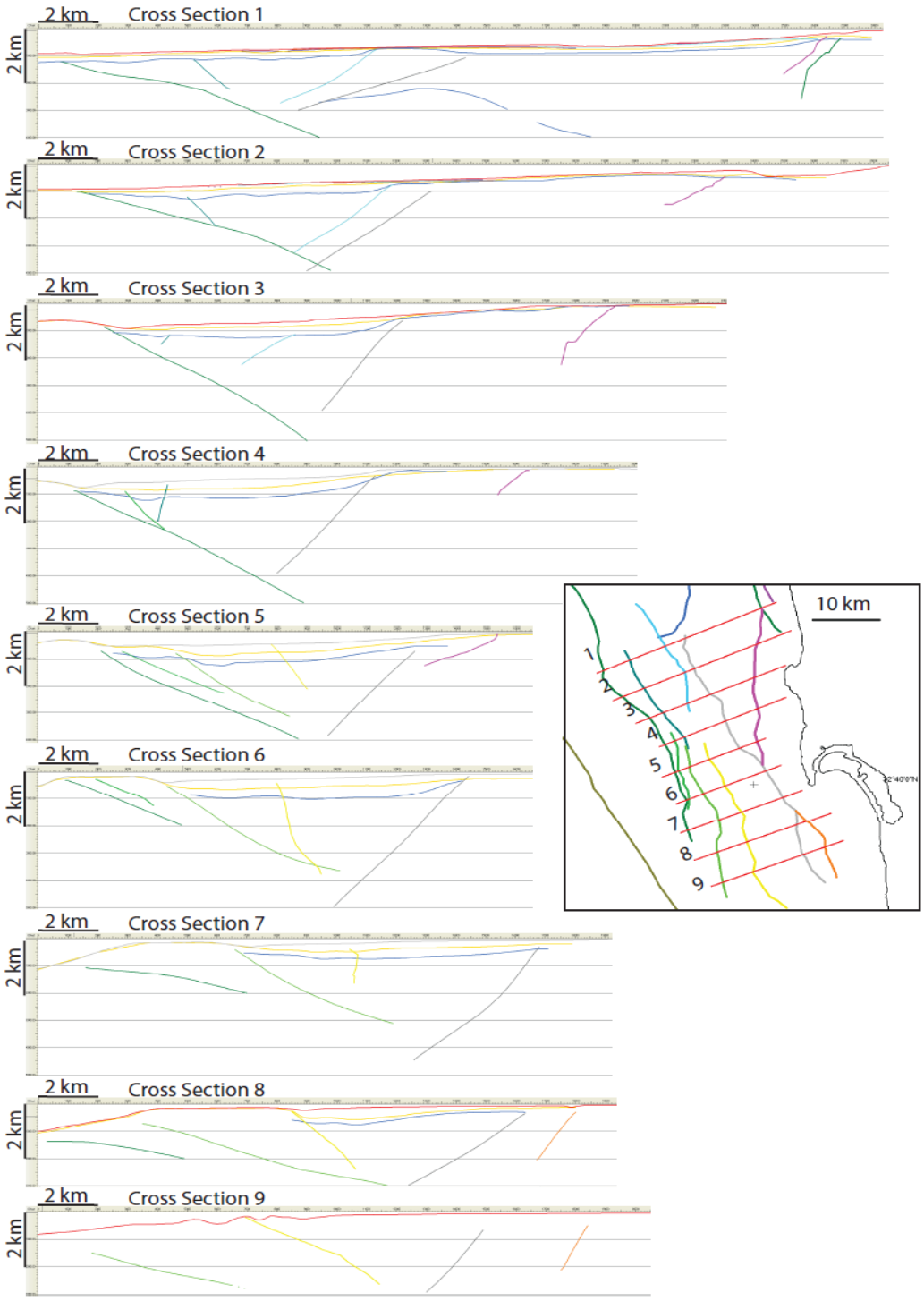


*Figure 22*: Cross sections with no vertical exaggeration across faults located south of the major right step over, including offshore San Diego. Cross Sections one through three show(from left) the Coronado Bank Detachment (dark green); Coronado(blue green); Carlsbad Splay 1(cyan); Descanso(gray); Slope Descanso Transfer (magenta); Coronado Splay 3(light green); Coronado Splay 4(yellow); and San Diego Shelf fault(orange). The location map provided shows how these faults develop and die out.

*4) Assessment of the nature and timing of the deformation of Quaternary sediments*

Isochore (vertical thickness) maps, shown in Figure 30, were produced from the depth- converted TLP and Q4 through Q1 sequence boundaries along with the seafloor. These maps illustrate that the locations of sediment accumulations in the ICB has changed frequently. Assessment of deformation of the Quaternary horizons was limited to deformation associated with the San Mateo-Carlsbad fault (Figures 15, 16, 21, and 22). Defining the age of these horizons provides increased accuracy for dating SMC-related deformation. TLP produced the greatest amount of contrast between positive (618 m) and negative (-170 m) relief. Q3 and Q4 relief were measured on cross sections 32-58 (inset map on Figure 21) and both exhibited similar relief patterns comparable to TLP, while exhibiting lower changes in relief (Figure 29).

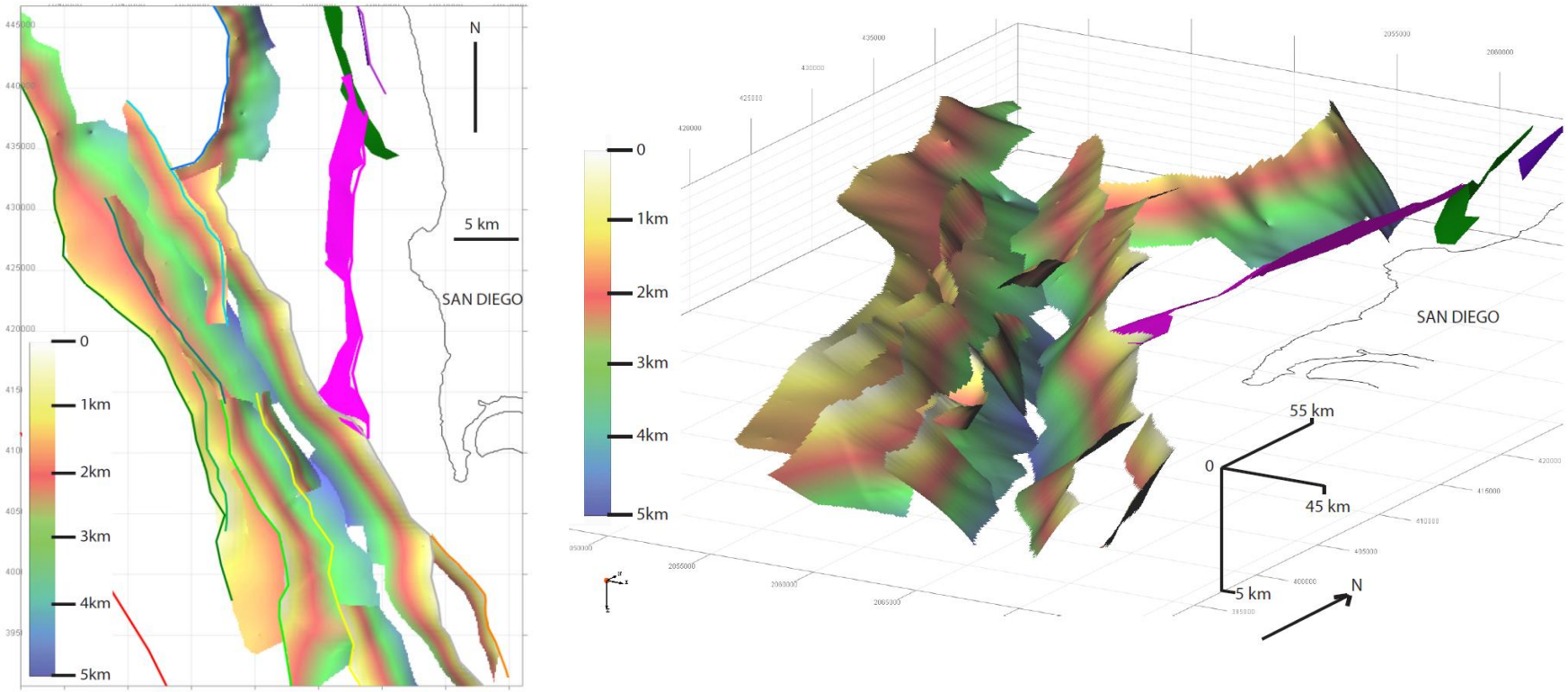


*Figure 23*: Right: A 3 dimensional rendering of depth converted fault surfaces, displayed with no vertical exaggeration. View to North-northwest. A consistent color scheme was applied to all faults so that they would be the same color for a given depth. This oblique perspective illustrates the major right step-over between the northern and southern flower structures. The southern faults display a left-stepping en-echelon pattern. The faults displayed in solid colors were too steep to grid and then depth convert using the 3D velocity model, given the modules available to us in the Kingdom Suite software. They were converted using single time depth charts I constructed using the Harvard velocity model. Refer to Figures 20 and 21 for the geometry of these and the other faults in cross section. Left: A map view of the same volume displayed at right. The upper edges of each fault are highlighted by curves with the same color as used in the fault map displayed in Figures 3 and 7.

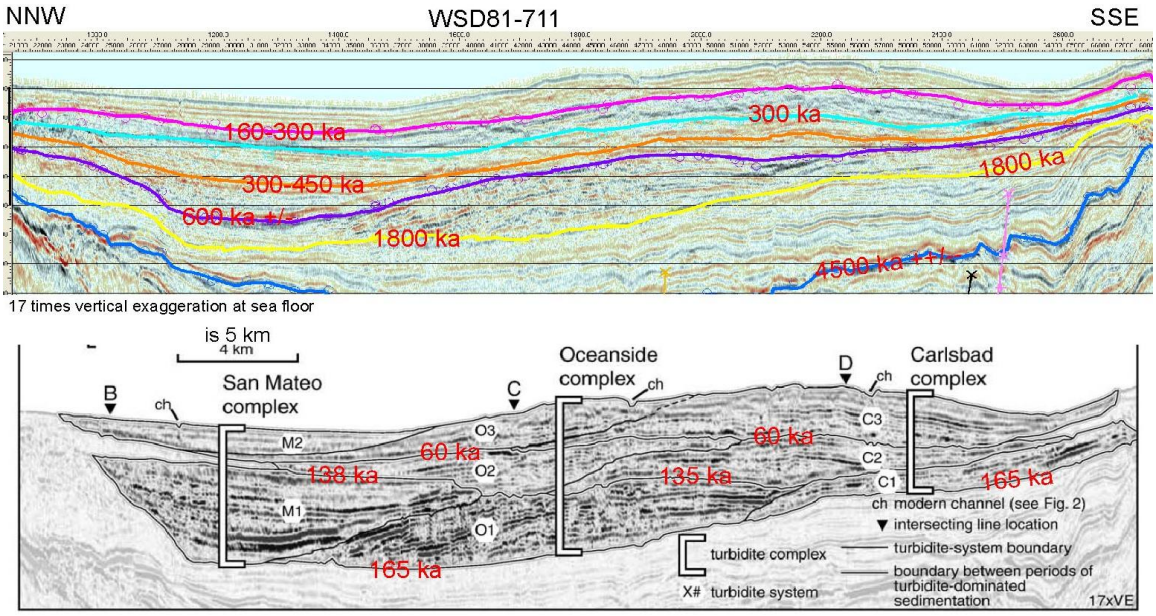


*Figure 24*: Above: Western Geophysical Company profile WSD 81-711shown with interpreted Quaternary 1 through H4 with ages provided from the scientific core hole at Pier F in Los Angeles harbor. This figure is also a part of the composite profile A-A' (Figure 18) showing the regional stratigraphic correlation completed for this study. Below: The same profile as above with interpreted ages by Covault and Romans (2009) for comparison. This is comparison is significant because such contrast in ages calculates different slip rates which is critical in assessing seismic hazard

*5) Measurement of the structural relief and modeling the sense and direction of displacement along one or more prominent ICB faults*

Prominent faults were interpreted throughout the study area, but structural relief and displacement modeling (predicted from fault strike, dip, and measured relief) could only be conducted where paleo-relief and initial dip were inferred to be minimal at the time of deposition. Patterns of stratal thinning across the San Mateo-Carlsbad fault indicate that the transition from Pliocene transtension to Quaternary transpression occurred about the time of an unconformity imaged between TLP and H4, and that little of the current sea floor relief had developed

by the time of TLP deposition. In addition, the horizons must be continuously interpreted in both the hanging-wall and footwall of the fault in order for displacement modeling to be possible using our trigonometric approach.

TLP is interpreted across the extent of the SMC fault and was used for the slip modeling in Sorlien et al. (2010). We use TLP again for modeling slip on the SMC fault after depth-converting this surface using the 80 time-depth charts from the SCEC Community Velocity Model. Reverse structural relief of the TLP ranges from 100 m to as much as 600 m in corridors 1 through 51. At the SMC step-over (or bend), we measured negative TLP relief greater than 100 m (Figure 25).

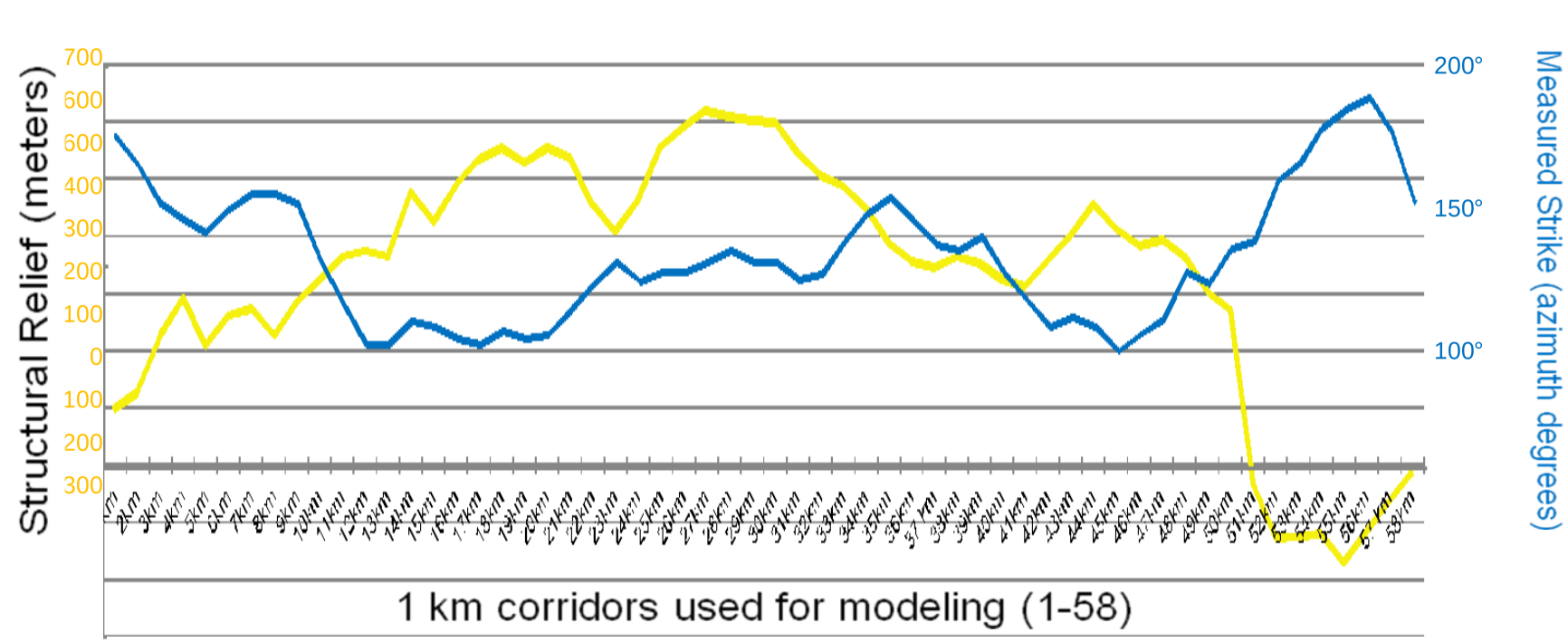


*Figure 25*: A line graph illustrating the relationship between San Mateo-Carlsbad (SMC) strike in azimuth degrees(Blue) and measured Top Lower Pico (TLP) vertical deformation in meters(yellow). Positive TLP relief is reported between corridors 3 and 50. TLP relief becomes negative after 51. We measured SMC strike values approaching 200 degrees which produces the step over/bend observed in map view. Negative TLP relief coinciding with this change of SMC strike indicates that the step-over/bend is releasing. A running average for strike values was used for the fault strike measurements since gridding and depth conversion increased the drastic changes in strike from each kilometer.

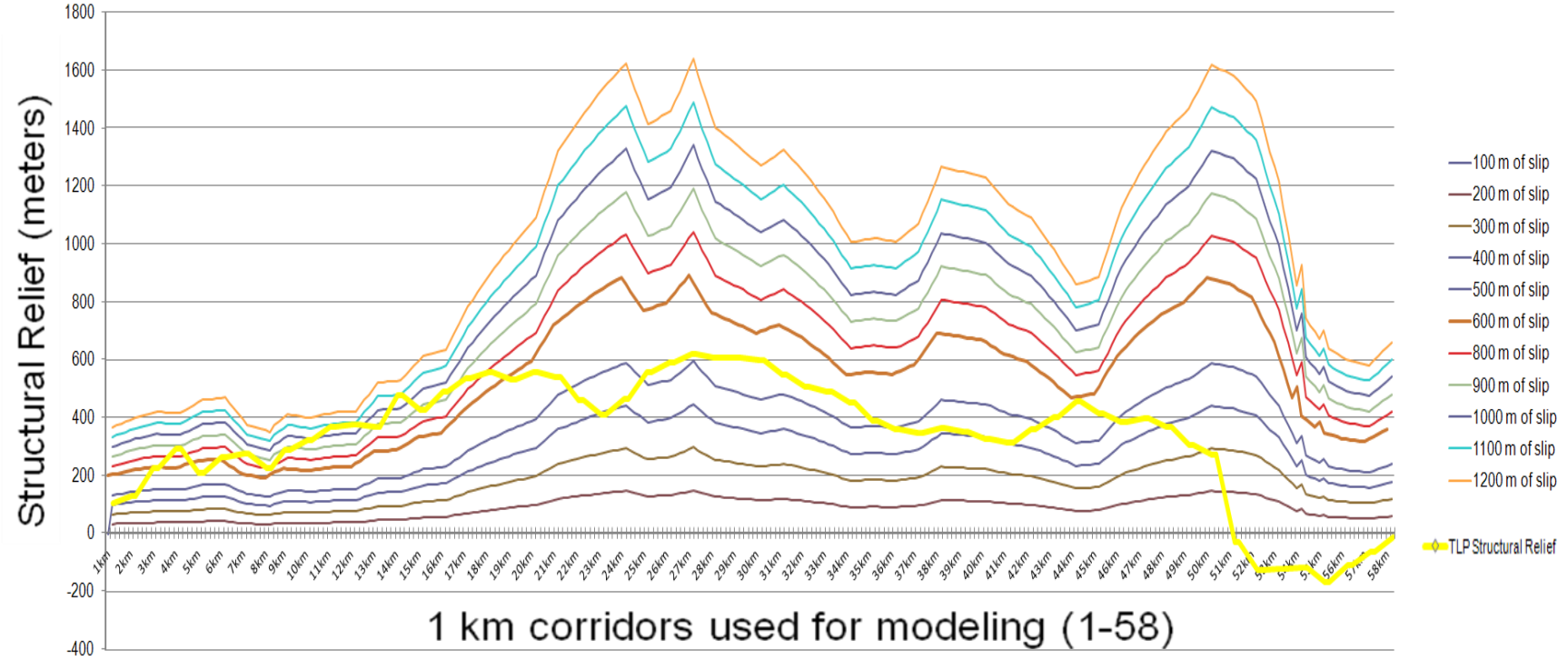


*Figure 26*: A line graph comparing modeled cumulative slip amounts with measured Top Lower Pico deformation (yellow) at an azimuth of 242˚ motion direction of the hanging wall block which is pure reverse motion. The modeling assumes that the measured vertical deformation is slip that is accumulating as rock passes through each 1 kilometer corridor. Measured TLP deformation does match well with pure reverse motion. This is significant since the San Mateo-Carlsbad fault responsible for this deformation is previously published as a thrust fault in Rivero et al. (2000).

Figure 26 shows modeled structural relief patterns for pure thrust motion (slip azimuth of 242°) compared to measured TLP structural relief. This comparison indicates that the measured vertical deformation of TLP south of the 14$^{th}$ km corridor simply does not match slip amounts relative to a slip direction of 242°. This contradicts previous studies, such as Rivero et al., (2000), that have interpreted the SMC as a blind thrust fault. However, the SMC fault is potentially a right-oblique thrust fault north of corridor 14, since the TLP deformation pattern coincides with the slip amounts at those corridors (Figure 26). SMC-induced deformation of TLP was also compared to a normal slip model of 62˚ (Figure 26). Only corridors 52-58 compared well to the lowest values 100-300 m.

The TLP deformation pattern best fits models with slip of the hanging wall block towards 162° through 177° (Figures 27 and 28). The cumulative slip average that best fits TLP relief is 0.79 km ± 0.2km. Assuming that TLP is correctly dated at 1.8 Ma (refer to the methods section and Figure 23) this implies the long-term average slip rate would be 0.5mm - 0.37mm per year. . This suggests that motion to the south along the SMC is more likely strike-slip.

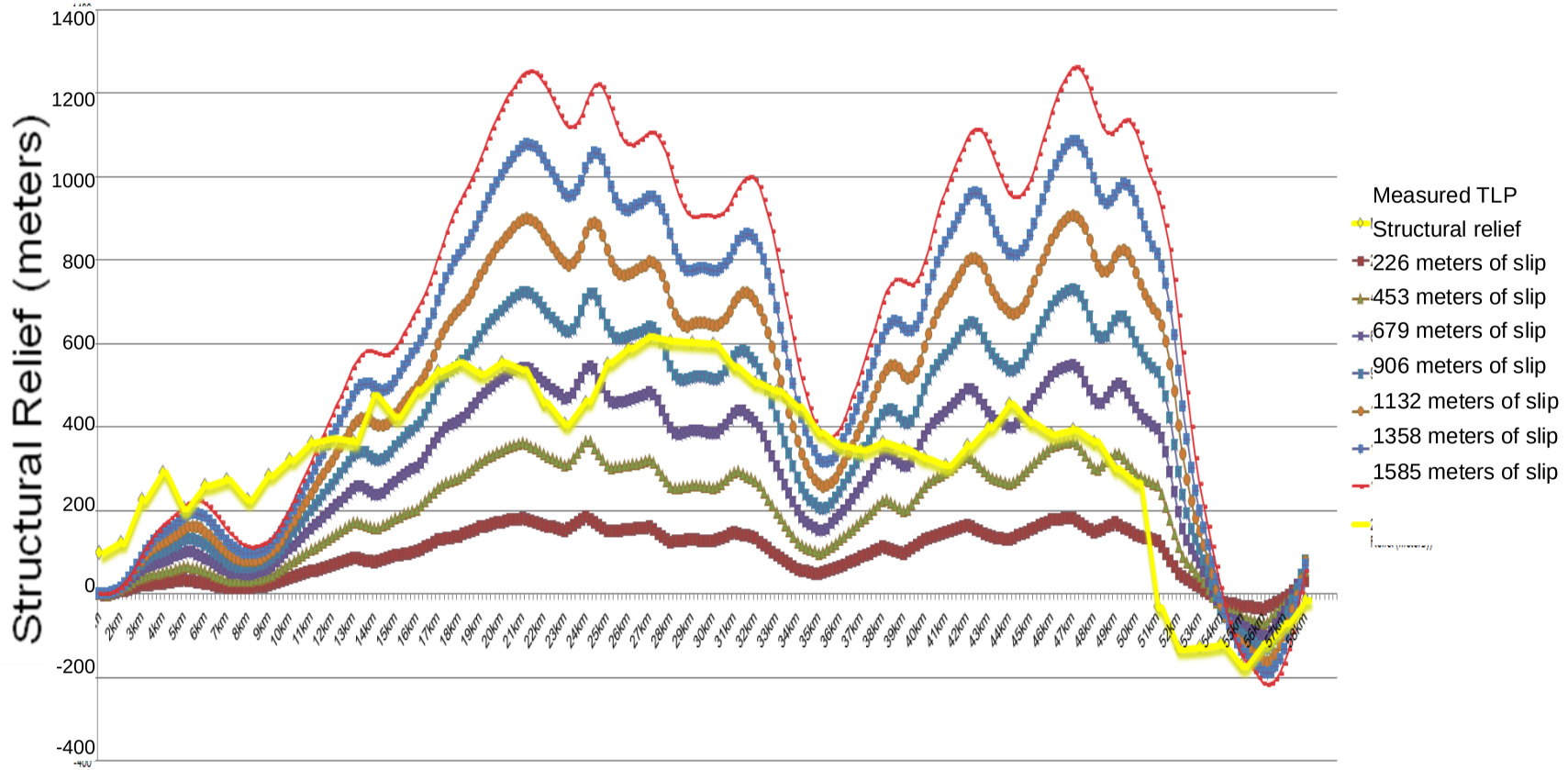


*Figure 27*: A line graph comparing an azimuth 162˚ motion of the hanging wall block with respect to the footwall block and measured top Lower Pico deformation. This motion orientation represents the lowest (in terms of azimuth degrees) best fit orientation with measured top Lower Pico (TLP) deformation (blue). The cumulative slip patterns for 679 and 906 meters match up best with pattern for measured TLP deformation.

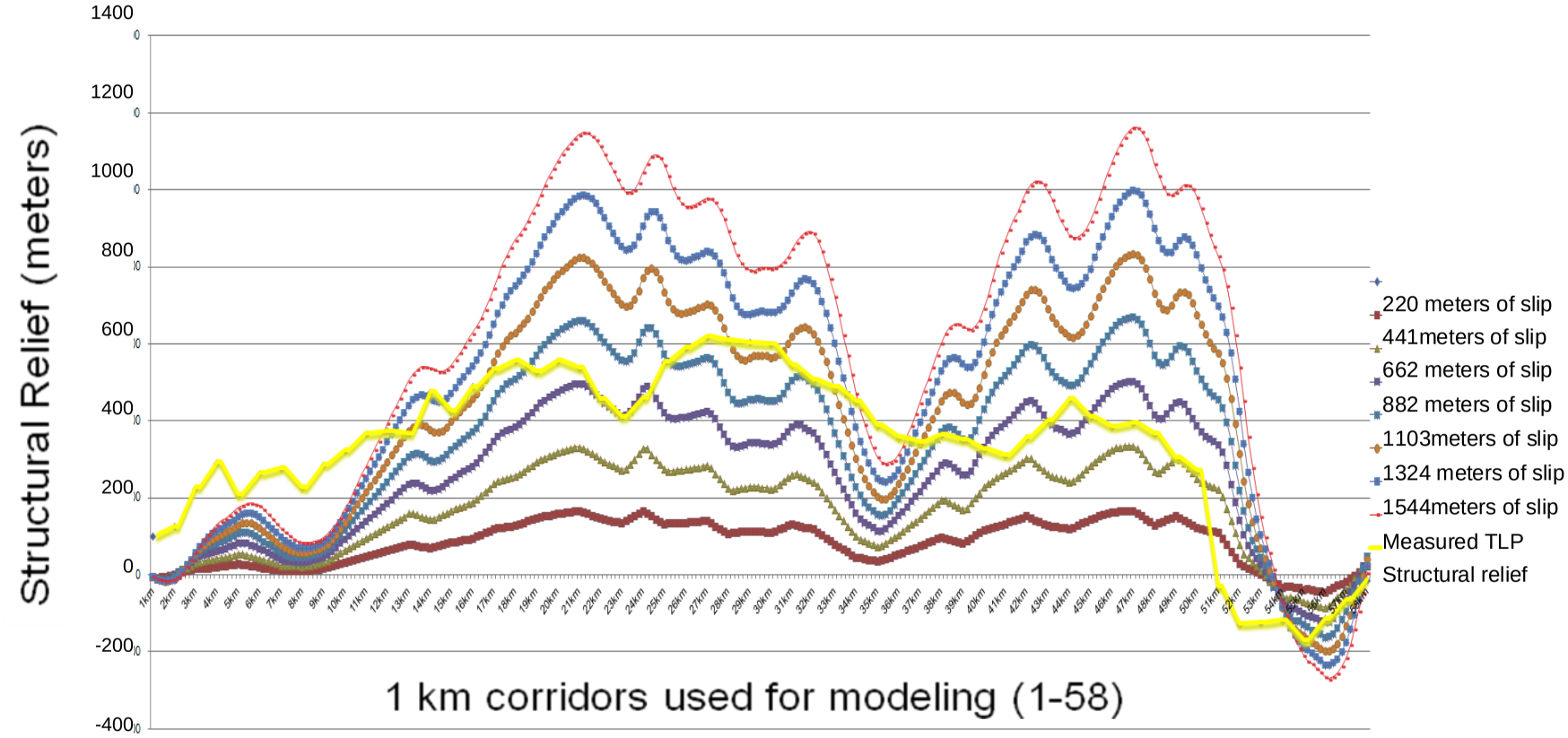


*FIGURE 28*: A line graph comparing an azimuth 177˚ motion of the hanging wall block with respect to the footwall block and top Lower Pico (TLP) deformation (yellow). This motion orientation is the greatest (in terms of azimuth degrees) best fit orientation with measured TLP deformation. The cumulative slip patterns for 679 meters match up best with pattern for measured TLP deformation. This amount is divided by 1,800,000 (age of TLP) to determine the average slip rate.

# CHAPTER 5: DISCUSSION

The products from this study detailed in the previous chapter include: new 3D representations of continuous fault systems in the ICB, kinematic evidence supporting a San Mateo-Carlsbad fault that is continuous for at least 58 km, and new age constraints on Quaternary sedimentation and SMC related deformation, and a mean slip rate on the SMC fault. This section discusses: 1) the implications of these results for the tectonic evolution of the ICB, 2) the significance of the slip rate estimates using my age model and slip rate estimates calculated using age models from previous studies, and 3) the history of Quaternary sedimentation in the ICB.

## Fault Geometry and Continuity

The seismic reflection profiles in Figures 13 and 14 show the San Mateo-Carlsbad-Newport-Inglewood faults and the Coronado Bank Detachment-Descanso faults converging at depth. Our interpretation of the northern and southern faults forming positive and negative flower structures respectively concurs with that of Ryan et al. (2009). The geometry of these faults may be in part dictated by pre-existing basement weaknesses that coincide with their convergence at depth.

However, in contrast to our mapping of the ICB faults, Ryan et al. (2009) mapped the faults as more segmented than continuous, and they did not map the Descanso fault. These differences are likely the result of the mapping criteria used to identify faults. Ryan et al. (2009) focused on defining Holocene-active faults and used a different dating method (described here in Chapter 2). We

mapped faults based upon how consistently they were identifiable in the seismic reflection profiles at depth. The Jennings et al. (2010) activity map presented faults that were previously published as active and presumably did not include interpretations based upon the multi-channel seismic reflection data released in first decade of the 21st century. This might explain why Ryan et al. (2009) mapped the San Mateo-Carlsbad fault as segmented and Jennings et al. (2010) did not recognize the large step-over of the SMC (e.g. Figure 7)

The ~10 km wide step over of the SMC fault to the Descanso fault documented in this study is critical to understanding how previous tectonic events impact fault activity in the present. It remains unclear whether this dilational or releasing step-over acts as a barrier for seismicity or if serves as a point of nucleation (Oglesby, 2005). The Oceanside thrust of Rivero et al. (2000) coincides with northern-most part of the SMC fault. They mapped their presumed Oceanside thrust fault to continue south, to coincide with our Coronado Bank detachment fault. Our analysis indicates that our northernmost San Mateo continues south-southeast where it coincides with the Carlsbad thrust of Rivero et al. (2000). The SMC fault is therefore more correctly identified as a right-oblique thrust fault that gradually behaves like a right-lateral strike-slip fault to the south (Figures 25, 27, 28). However, it remains unclear if the Descanso fault is a continuation of the SMC fault.

Measurements of structural relief across the SMC fault (predominantly positive) document that this step-over marks a boundary between transpression in the north and transtension in the south. While this step-over/bend may be

related to some pre-existing basement weaknesses, it remains unclear whether transpression will migrate south over time or if transtensional forces will dominate the southern ICB over time.

**San Mateo-Carlsbad Kinematics and Slip Rate**

Simple geometrical modeling is applied to predict the vertical deformation that would result across the SMC fault for a range of slip direction and range of cumulative slip. Slip amount and direction were estimated for the SMC fault by comparing the modeled deformation to the deformation measured in this study (refer to the Data and Methods of Analysis and Results chapters for more detail on the modeling).

Because our geometrical modeling of the vertical deformation across a continuous SMC fault can reproduce the observation, it supports the contention that this fault is kinematically continuous. This adds confidence to our MCS interpretation and subsequent mapping of the SMC as continuous rather than segmented.

The slip rate of 0.5mm - 0.37mm/yr due south for the SMC fault is based upon the 1800 ka age constrained by Sorlien et al. (2010). In contrast, Covault and Romans' (2009) date of ~165 ka (Figure 24) for a horizon above our 1800 ka TLP yields a mean slip rate as high ~6mm/yr (more than an order of magnitude faster than we propose), a slip rate comparable to that of some notoriously hazardous strike-slip faults. For example, a rate of 6 mm/yr is attributed to the Enriquillo-Plantain Garden Fault that ruptured catastrophically in Haiti in January 2010, causing more than 230,000 fatalities (Calais et al, 2010)Thus, this discrepancy is very significant to future studies assessing hazard posed by ICB faults. The high contrast in ages for horizons near the same depth highlights the importance in understanding sedimentation patterns throughout the Quaternary in the ICB.

**Quaternary Sedimentation**

The isochore maps in Figure 30 clearly show that the locations of sediment accumulation shift over time but remain in the footwall of the SMC fault. Areas of increased thickness coincide with the locations of turbidite complexes interpreted by Covault and Romans (2009) (Figure 8). This adds support to our Q horizon interpretations even though our focus was not to interpret the extent of turbidite complexes. This varied sedimentation suggests that extrapolating below core data to constrain ages is not a reliable approach.

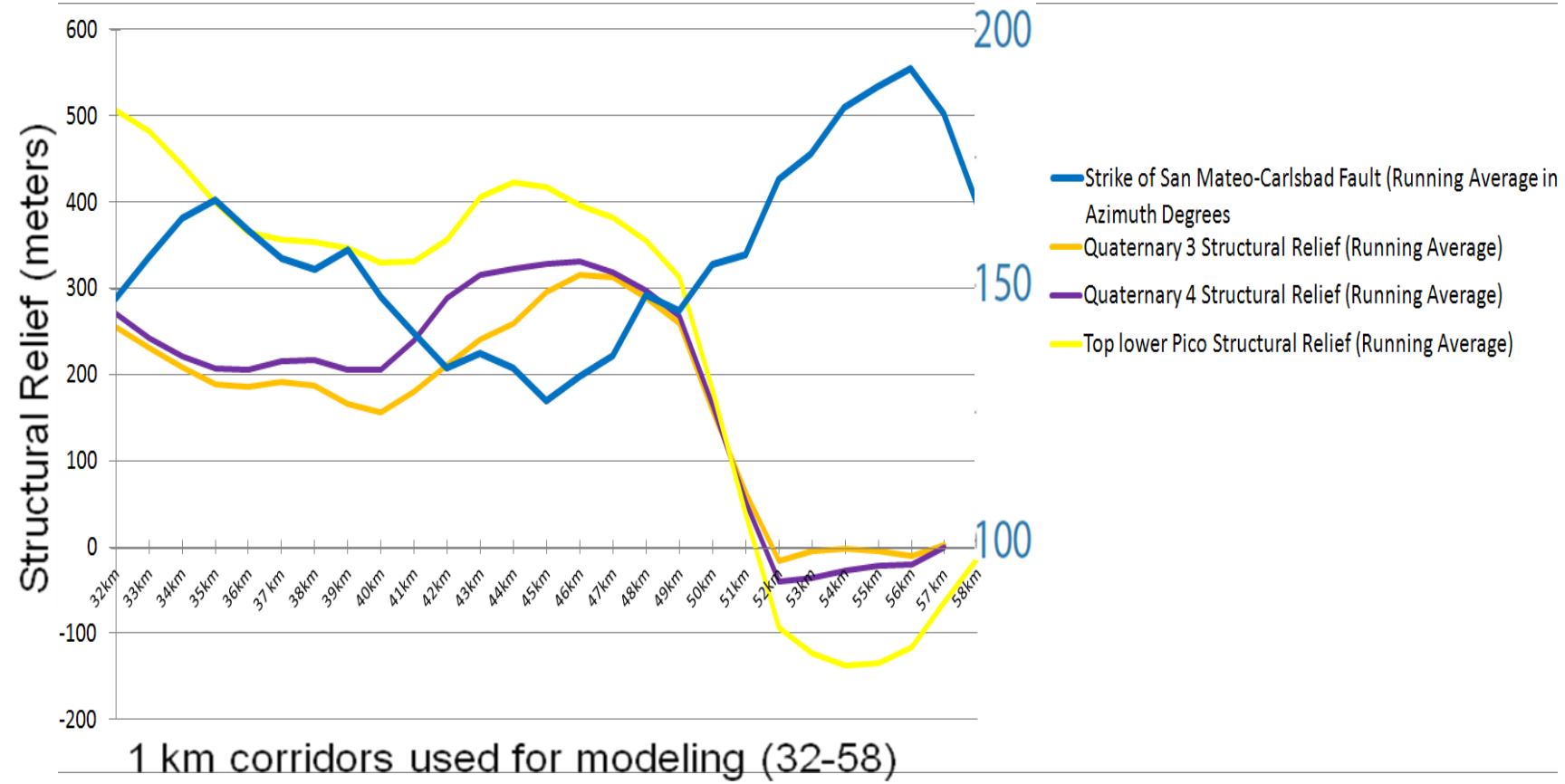


*FIGURE 29*: A line graph comparing measured Quaternary 3 (orange), 4 (violet) and top Lower Pico TLP (yellow) vertical deformation against the strike (blue) of the San Mateo-Carlsbad fault. Measured deformation for the Quaternary horizons is progressively less than that of TLP. The amount of relief decreases over time suggests that activity in the San Mateo Carlsbad fault is decreasing over time as well. The Quaternary horizons could not be interpreted over the entire 58 cross sections. This is probably due to on lapping and varied sedimentation over time. Running averages were computed for each value presented here to resolve value shifts produced from gridding and depth conversion.

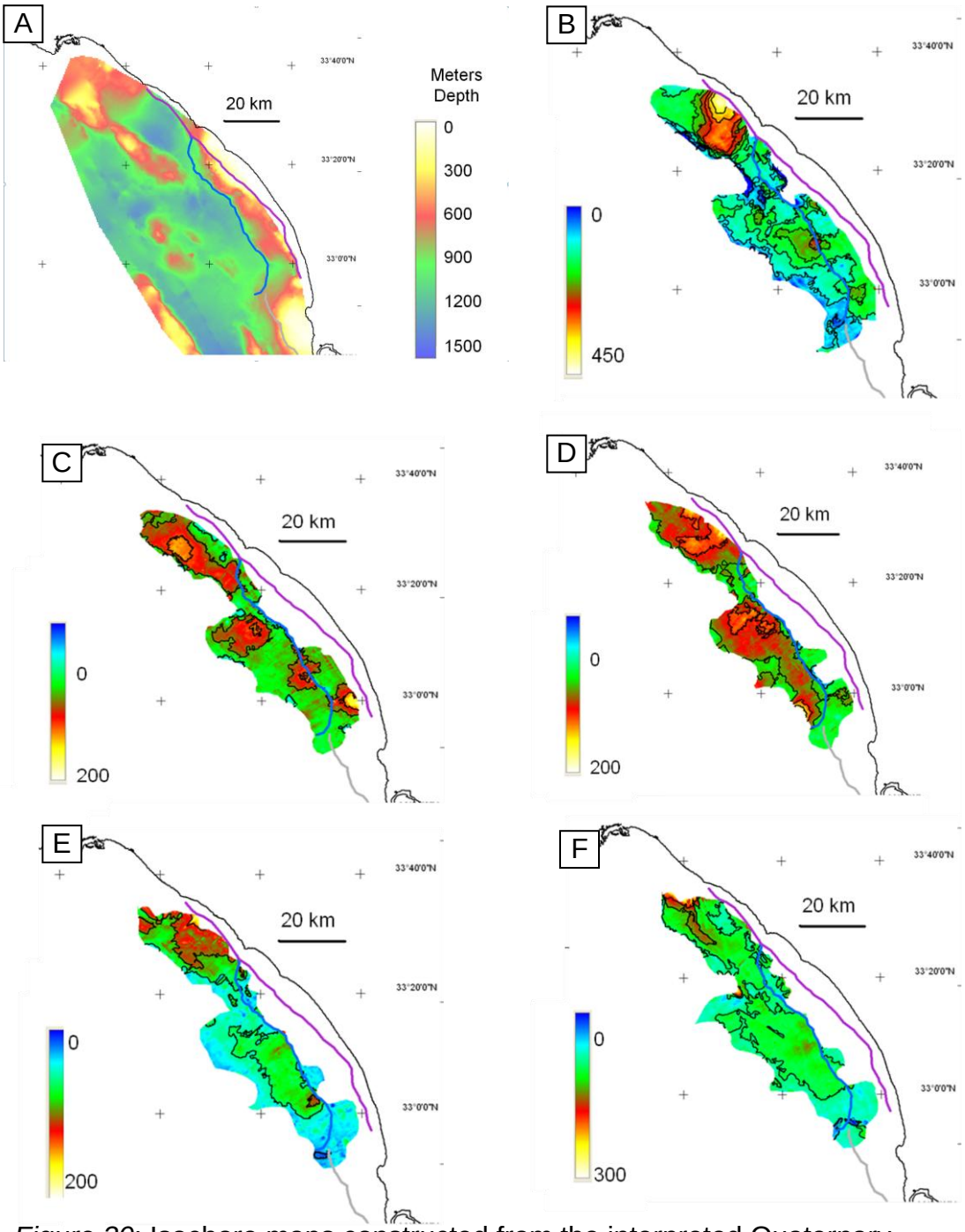


*Figure 30*: Isochore maps constructed from the interpreted Quaternary horizons. Map A is gridded surface of Top lower Pico. Map B shows the difference between Top Lower Pico and Quaternary 4; C shows Quaternary 4 versus Quaternary 3; D shows Quaternary 3 versus Quaternary 2; E Shows Quaternary 2 versus Quaternary 1 and F shows Quaternary 1 versus the seafloor. Areas with increased thickness indicate that locations of sediment accumulation did not remain constant. This is problematic for dating techniques used by Normark et al. (2009) since it does not address these possible sedimentation shifts.

## Proposed Future Work

Controversies surrounding Quaternary faults and stratigraphy in the ICB can be resolved in future studies by establishing and consistently implementing the same fault identification and activity criteria. There would be less uncertainty when assessing the validity of work done to generate fault maps and allows for more emphasis to be placed on the quality and thoroughness of interpretation.

Additional high-resolution and deep crustal seismic reflection data are needed to verify the findings presented in this study. A greater density in high resolution data would allow for workers to conduct their own stratigraphic interpretations in the Quaternary ICB stratigraphy, which would potentially add confidence to the stratigraphy and dating correlation documented in this study. Deep-crustal seismic reflection data would better image the SMC, NI, CBD, and Descanso faults, potentially resolving cross-cutting or merging geometries among the faults and the influence of pre-existing weaknesses on quaternary faulting.

Additional high-resolution seismic reflection data is needed to better image the step-over/bend and associated faults documented in this study. Such data would resolve whether the SMC fault steps over to the right or bends, merging with the Descanso fault to the south.

## CHAPTER 6: CONCLUSIONS

The analysis of ICB multi-channel seismic reflection data provided a foundation upon which great confidence could be placed on the depth converted fault surfaces and horizons so that measurements used for slip modeling could be taken. The conclusions that are drawn from the subsequent results should provide new insight into the geology found offshore southern California as detailed in the previous chapter. What follows in this chapter is a list of the conclusions from this study.

1.) The ~9 km wide step-over/bend in the SMC fault marks the southern extent of transpression and northern extent of transtension observed in the ICB.

2.) The SMC fault is modeled as kinematically continuous with a slip direction of the northeast hanging-wall relative to the footwall towards an azimuth ranging from 162˚ to 177˚. The average slip rate is 0.4-0.5 mm/year since ~1.8 Ma..

3.) The SMC-Newport-Inglewood positive flower structure steps right ~19 km over to the Coronado Bank-Descanso negative flower structure. This major step-over may act to arrest an earthquake rupture, thus limiting the likely maximum earthquake magnitudes.

4.) The right step-over between the northern and southern fault system flower structures, which spatially coinciding with the transition between transpression and transtension, is consistent with right-lateral strike-slip.

5.) Isochore maps indicate that sedimentation was not constant and depocenters have shifted spatially throughout the Quaternary. Sequence

boundaries, such as the ~600 ka Q4, can locally represent hundreds of meters of missing section rather than one 100 ka climate cycle.

6.) Using our new age model for Quaternary stratigraphy, slip rates on the San-Mateo Carlsbad fault, and thus earthquake hazard, are an order of magnitude lower than suggested by a recently-published age model.

# BIBLIOGRAPHY

Atwater, T., 1970, Implications of plate tectonics for the Cenozoic tectonic evolution of western North America: Geological Society of America Bulletin, v. 81, p. 3513-3536.

Atwater, T., and Stock, J., 1998, Pacific-North American plate tectonics of the Neogene southwestern United States An update: International Geology Review, v. 40, p. 375-402.

Beavan, J., Tregoning, P., Bevis, M., Kato, T., and Meertens, C., 2002, Motion and rigidity of the Pacific Plate and implications for plate boundary deformation, J. Geophys. Res., 107(B10), 2261, doi:10.1029/2001JB000282

Calais, E., A. M. Freed, G.S. Mattioli, F. Ameling, S. Jonsoon, P. Jansma, S.-H. Hong, T.H. Dixon, C. Prepetit, and R. Momplaisir, (2010). "Transpressional rupture of an unmapped fault during the 2010 Haiti earthquake." Nature Geoscience 3(11): 794-799.

Campbell, B. A., C. C. Sorlien, M.-H. Cormier, and W. S. Alward, 2009, Quaternary deformation related to the 3D geometry of the Carlsbad fault, offshore San Clemente to San Diego, Southern California Earthquake Center Annual Meeting, Proceedings and Abstracts v. XIX poster 2-025, p. 263-264.

Covault, J.A., and Romans, B.W., 2009, Growth patterns of deep-sea fans revisited: Turbidite-system morphology in confined basins, examples from the California Borderland: Marine Geology, v. 265, p. 51-66.

Crouch, J.K., and Suppe, J., 1993, Late Cenozoic tectonic evolution of the Los Angeles basin and inner California borderland: A model for core complex-like crustal extension: Geological Society of America Bulletin, v. 105, p. 1415-1434.

Crowell, J. C., 1979, The San Andreas fault system through time, Journal of the Geological Society London, vol. 136, p.293-302

Dartnell and Gardener 1999, Sea-Floor Images and Data fro Multibeam Surveys in San Francisco Bay, Southern California, Hawaii, the Gulf of Mexico and Lake Tahoe, California-Nevada Geological Survey.

Dixon, T., Farina, F., DeMets, C., Suarez-Vidal, F., Fletcher, J., Marquez-Azua, B., Miller, M., Sanchez, Osvaldo, Umhoefer, P., 2000, New kinematic models for Pacific-North America Motion from 3 Ma to Present, II: Evidence for a “Baja California Shear Zone”: Geophysical Research Letters, v. 27 n. 23, p. 3961, doi: 1029/2000GL008529

Fisher, M.A., Langenheim, V.E., Nicholson, C., Ryan, H.F., and Sliter, R., 2009, Recent developments in understanding the tectonic evolution of the southern California offshore area: Implications for earthquake hazard analysis *in* Lee, H.J., and Normark, W.R., eds., Earth Science in the Urban Ocean: the Southern California Continental Borderland: Geological Society of America Special Paper 454, p. 229-250.

Gorsline, D.S., 1992, The geological setting of Santa Monica and San Pedro Basins, California Continental Borderland: Progress in Oceanography, v. 30, p. 1-36.

Hart, P. E. and J. R. Childs, 2005, National archive of marine seismic surveys (NAMSS): Status report on U. S. Geological Survey program providing access to proprietary data, *Eos Trans. AGU, 86*(18), Jt. Assem. Suppl., Abstract S41A-10, http://walrus.wr.usgs.gov/NAMSS/

Jennings, C. W, W. A. Bryant, and G. Saucedo, 2010, Fault activity map of California, California GeologicalSurvey http://www.consrv.ca.gov/cgs/cgs_history/PublishingImages/FAM_750k_MapRelease_page.jpg

Legg, M.R., 1991, Developments in understanding the tectonic evolution of the California Continental Borderland, *in* Osborne, R.H. ed., From shoreline to abyss: Contributions in marine geology in honor of Francis Parker Shepard: Tulsa, Oklahoma, Society of Economic Paleontologists and Mineralogists Special Publication 46, p. 291–312.

Lisiecki, L.E., Raymo, M.E., 2005, A Plio-Pleistocene Stack of 57 Globally Distributed Benthic $\delta^{18}O$ Records: Paleoceanography, vol. 20, PA1003 doi:10.1029/2004PA001071

Kamerling, M., and Luyendyk, B. P., 1985, Paleomagnetism and Neogene tectonics of the northern Channel Islands, California, Journal of Geophysical Research, vol. 90, no. B14, p. 12485-12502

Luyendyk, B.P., 1991, A model for Neogene crustal rotations, transtension, and transpression in southern California: Geological Society of America Bulletin, v. 103, p. 1528-1536.

Lyle, M., Koizumi, I., Richter, C. and others, 1997, Initial reports, Ocean Drilling Program, Leg 167: College Station, Texas, Ocean Drilling Program, p. 157-174.

Nicholoson, C., Sorlien, C.C., Atwater, T., Crowell, J.C., and Luyendyk, B.P., 1994, Microplate capture, rotation of the western Transverse Ranges, and initiation of the San Andreas transform as a low-angle fault system: Geology, v. 22, p. 491-495.

Normark, W.R., McGann, M., and Sliter, R.W., 2009, Late Quaternary sediment-accumulation rates within the inner basins of the California Continental Borderland in support of geologic hazard evaluation *in* Lee, H.J., and Normark, W.R., eds., Earth Science in the Urban Ocean: the Southern California Continental Borderland: Geological Society of America Special Paper 454, p. 117-139.

Oglesby, D.D., 2005, The Dynamics of Strike-Slip Step-Overs with Linking Dip-Slip Faults: Bulletin of the Seismological Society of America, v. 95, n. 5 p. 1604-1622, doi:10.1785/0120050058

Plesch, A, J. H. Shaw, C. Benson, W. A. Bryant, S. Carena, M. Cooke, J. Dolan, G. Fuis, E. Gath, L. Grant, E. Hauksson, T. Jordan, M. Kamerling, M. Legg, S. Lindvall, H. Magistrale, C. Nicholson, N. Niemi, M. Oskin, S. Perry, G. Planansky, T. Rockwell, P. Shearer, C. Sorlien, M. P. Suss, J. Suppe, J. Treiman, and R. Yeats, Community Fault Model (CFM) for southern California, Bulletin of the Seismological Society of America, V. 97, p. 1793-1802, DOI: 10.1785/0120050211

Ponti, D.J., Ehman, K.D., Edwards, B.D., Tinsley, J.C., Hildenbrand, T., Hillhouse, J.W., Hanson, R.T., McDougall, K., Powell, C.L., Wan, E., Land, M. Mahan, S., Andrei, M., Sarna Wojcicki., 2007, A 3-Dimensional Model of Water-Bearing Sequences in the Domin guez Gap Region, Long Beach, California, America Special Paper 454, p. 141-168. United States Geological Survey Open-File Report 2007-1013, 34p.

Rivero, C., Shaw, J.H., and Mueller, K., 2000, Oceanside and Thirtymile Bank blind thrusts: Implications for earthquake hazards in coastal southern California: Geology, v. 28, p. 891-894.

Rivero, C., and J.H. Shaw, 2011, Active folding and blind thrust faulting induced by basin inversion processes, inner California borderlands, in K. McClay, J.H. Shaw, and J. Suppe, eds., Thrust fault-related folding: American Association of Petroleum Geologists Memoir 94, p. 187 – 214.

Ryan, H.F., Legg, M.R., Conrad, J.E., and Sliter, R.W., 2009, Recent faulting in the Gulf of Santa Catalina: San Diego to Dana Point, *in* Lee, H.J., and Normark, W.R., eds., Earth Science in the Urban Ocean: the Southern California Continental Borderland: Geological Society of America Special Paper 454, p. 291-315.

Suess, M. P., and J. H. Shaw, 2003, P-wave seismic velocity structure derived from sonic logs and industry reflection data in the Los Angeles basin, California, JournalofGeophysicalResearch,108/B3.

Sorlien, C.C., Campbell, B.A., and Seeber, L., 2010, Geometry, kinematics and activity of a young mainland-dipping fold and thrust belt: Newport Beach to San Clemente, California: United States Geological Survey External Research Paper 08HQGR0103, 25 p.

Sylvester, A.G., 1988, Strike-slip faults: Geological Society of America Bulletin, v. 100, p.1666-1703

Warrick, J.A., and Farnsworth, K.L., 2009, Sources of sediment to the coastal waters of the Southern California Bight *in* Lee, H.J., and Normark, W.R., eds., Earth Science in the Urban Ocean: the Southern California Continental Borderland: Geological Society of America Special Paper 454, p. 39-52.

Warrick, J.A., and Farnsworth, K.L., 2009a, Dispersal of river sediment in the Southern California Bight, *in* Lee, H.J., and Normark, W.R., eds., Earth Science in the Urban Ocean: the Southern California Continental Borderland: Geological Society of America Special Paper 454, p. 53-67.

Wilson, D.S., McCory, P.A., and Stanley, R.G., 2005, Implications of volcanism in coastal California for the Neogene deformation history of western North America: Tectonics, v. 24, TC3008, p. 1-22.

Wright, T.L., 1991, Structural geology and tectonic evolution in the Los Angeles Basin, California, in K.T. Biddle, ed., Active Margin Basins, AAPG Memoir 52, American Association of Petroleum Geologists, Tulsa, p.35-135